DEGREE PROJECT IN THE BUILT ENVIRONMENT,
SECOND CYCLE, 30 CREDITS
STOCKHOLM, SWEDEN 2018

Slope stability assessment through field monitoring

YUKUN WEI

KTH ROYAL INSTITUTE OF TECHNOLOGY
SCHOOL OF ARCHITECTURE AND THE BUILT ENVIRONMENT

Slope stability assessment through field monitoring

YUKUN WEI

Master Thesis, 2018
KTH Royal Institute of Technology
School of Architecture and the Built Environment
Department of Civil and Architectural Engineering
Division of Soil and Rock Mechanics
SE-100 44, Stockholm, Sweden

TRITA KRV Report 14/06 [TRITA-ABE-MBT-18477]
ISSN 1100-7990
ISRN KTH/KRV/14/06-SE
ISBN 978-91-7595-367-0

Abstract

Deterministic methods have been used in geotechnical engineering for a long period, such as slope stability calculations. However, only applying deterministic methods is subjective and imperfect. There is a demand to develop a systematic methodology to link the assessed slope stability and field measurement data, which is also known as inverse analysis and forward calculation.

Based on the Nya Slussen project, this thesis includes the development of a methodology, deterministic calculation for 4 cross sections using finite element program Plaxis 2D and probabilistic calculation for one section. Deterministic analyses showed satisfying results for all the studied cross sections since their factors of safety exceeded the minimum requirement. In probabilistic design, three parameters were found to have the most uncertainties through sensitivity analysis (undrained shear strength of clay, Young's modulus of clay and friction angle of fill). Inverse analysis was done by testing different values of them in Plaxis and to try to match the displacement components provided by field measurement. After finding the best optimization for all the parameters, forward calculation gave a final factor of safety. It is suggested that both of the methods should be utilized together for better assessment.

Keywords

Slope stability, inclinometer, displacement, FEM, inverse analysis.

Sammanfattning

Deterministiska metoder har använts inom geotekniken under lång tid, såsom släntstabilitetberäkningar. Dessa beräkningar är dock behäftade med subjektiva bedömningar och stor osäkerhet. Det finns ett behov av att utveckla en systematisk metodik för att koppla utvärderingen av släntstabilitet med fältmätningar. Detta kan göras med ’inverse analysis’ och ’forward calculation’.

I samband med den nya Slussen projektet, innefattar detta examensarbete utvecklingen av metodik, deterministiska beräkningar för 4 sektioner med FEM programmet Plaxis 2D och probabilistisk beräkning för en sektion. Deterministiska analyser visade tillfredsställande resultat för alla sektioner, eftersom de utvärderade säkerhetsfaktorerna översteg gränsvärdet. I de probabilistiska analyserna hittades tre parametrar genom känslighetsanalys som hade störst osäkerheter (odränerad skjuvhållfasthet för lera, Youngs E-modulus för lera och friktionsvinkel för fyllning). Omvända analyser utfördes genom att testa olika värden av dem i numerisk modellering och försöka finna värdena som kan koppla dem med uppmätta faktiska rörelser. Efter att den bästa optimeringen hittats, gav de främre beräkningarna den slutliga uppdaterade säkerhetsfaktorn. Det föreslås att både deterministiska och probabilistiska metoder används parallellt för en bättre utvärdering av släntstabiliteten.

Nyckelord

Släntstabilitet, inklinometer, rörelse, FEM, omvänd analys.

Preface / Acknowledgements

This thesis is considered as the last part of my master's study at Civil and Architectural Engineering at KTH. The idea of this thesis was proposed by ELU Konsult AB. It has been almost six months since I started my thesis work at ELU Konsult AB. I would like to thank all the talented and nice people from geotechnical department for your kind help during my thesis period, especially my supervisor Anders Beijer-Lundberg for your teaching, guidance and encouragement.

I would also like to thank my supervisor Stefan Larsson at KTH for your valuable suggestions and comments. Finally, thanks very much to all the people who have been supporting me at KTH.

Stockholm, June 2018
Yukun Wei

Nomenclature

Abbreviations

LOAD Load and resistance factor design
CS Cross section
FS Factor of safety
PEM Point estimate method
FOSM First Order Second Moment Method
FORM First Order Reliability Method
SORM Second order reliability method
MCS/MCM Monte Carli simulation/method
FEM Finite element method
RFEM Random finite element method
TDR Time domain reflectometry
FBG Fiber Bragg Grating
EBM Extended Bayesian method
LSM Least square method
MLM Maximum likehood method
WLSM Weighted least square method

Latin Symbols

R	Resistance	$[kN]$
S	Load effect	$[kN]$
$Var[x]$	Variance	
$Cov[x]$	Coefficient of variation	
$C_x(r)$	Autocovariance	
$P_{\pm\pm\pm}$	Weight factor	
E	Young's Modulus	$[MPa]$
a	Factor for parameter 1	
b	Factor for parameter 2	
c	Factor for parameter 3	
c'	Soil cohesion	$[kPa]$
E_{50}^{ref}	Secant stiffness from triaxial	$[MPa]$
E_{oed}^{ref}	Tangent stiffness from oedometer	$[MPa]$
E_{ur}^{ref}	Unloading reloading stiffness	$[MPa]$
m	Power	
e_{ini}	Initial void ratio	

$k_x\ k_y$	Permeability	$[m/s]$
c_u	Undrained shear strength	$[kPa]$
$L_{spacing}$	Distance between soil nailings	$[m]$
T_{skin}	Maximum compression/tension force	$[kPa]$

Greek Symbols

σ	Standard deviation/stress	[none/kPa]
μ	Mean value	
γ_1	Skewness	
$\rho_{x,y}$	Pearson correlation coefficient	
β	Reliability index	
ε	Strain	
β_i	Weight factor for inclinometer	
δ_{mea}	Measured displacement	$[mm]$
δ_{cal}	Calculated displacement	$[mm]$
$\Delta\delta$	Difference between δ_{mea} and δ_{cal}	$[mm]$
θ	Model parameter	
γ_{uns}	Unsaturated unit weight	$[kN/m^3]$
γ_{sat}	Saturated unit weight	$[kN/m^3]$
φ	Friction angle	[°]
ψ	dilatancy angle	[°]
υ	Poisson's ratio	
δ_y	Vertical displacement	$[mm]$
δ_x	Horizontal displacement	$[mm]$
α	Angle between Slope R1 and North	[°]
φ_{fill}	Friction angle of fill	[°]

Contents

1. Introduction

Slope stability is normally an important geotechnical task during construction, which includes excavations and changes in load or groundwater conditions. It is therefore a significant feature of practical geotechnical design. Regarding the safety requirements, extensive monitoring of soil deformation and pore pressure is sometimes carried out throughout the construction procedure.

Traditionally, those measurement data are interpreted or computed by empirical methods that mainly come from practical experience. For instance, deterministic stability analysis illustrated by Load and Resistance Factor Design (LRFD) is carried out to determine a specific safety factor prior to excavation. It represents a safety level to guide all construction activities. Alternatively, probabilistic methods can be used as a tool for slope stability assessment since it provides greater transparency by taking the variability of governing parameters into account and it gives a reliability index for the project. Both methods give similar practical result for most of the slopes such as maximum load, excavated geometry and excavation order.

However, there are great uncertainties remaining if only those methods are used. Sometimes field measurements related to slope stability need to be analyzed in a more systematic and thorough way to relate the field measurements to these methods. A methodology of risk assessment is then needed to analyze the huge amount of real-time measurement data given by extensive monitoring. In this thesis, the system should include back analysis (inverse analysis) and forward calculation. Several chosen parameters on site were calculated inversely with respect to measurement data and the new values were calculated forwardly to reach a final factor of

safety. Therefore, such a systematic system for slope stability assessment is under great demand and it would be a useful tool for the industry.

1.1. Aims

The main purpose of this thesis is to develop a systematic approach for slope stability assessment through field monitoring, which can provide suggestions for future practical projects.

1.2. Scope

Based on an instrumented slope of an ongoing project in Slussen Stockholm, the interaction between recorded field measurements and slope stability is explored by a deterministic method and a probabilistic method. Inverse analysis is needed in such a system to relate the measurements to the stability of the slope. Moreover, the slope has been modelled and analyzed by numerical modelling program Plaxis 2D. Comparisons between conventional method and proposed system are discussed in this thesis.

1.3. Content

In this thesis, different parts of the project are presented:

Introduction: A general introduction of background along with descriptions of currently used method for slope stability assessment are given along with aim, scope and an overview of content.

Literature survey: Based on previous project and publications, a literature research has been carries out. General definition of slope stability is discussed at first followed by several numerical modelling methods and field monitoring approaches.

Methodology: Traditional deterministic method and probabilistic method (reliability based) are introduced. Then an assessment methodology is proposed after completing statistical analysis and inverse calculation of monitoring data.

Case study and Result (deterministic method): A case study is discussed based on a slope in Slussen Stockholm. Geological conditions and geometry of the slope is first shown in the section. Then the field monitoring system as well as calculation methods are described. In order to generalize this case, an idealization is made to simplify the geometry, loads and soil parameters. A deterministic factor of safety before field monitoring states is calculated.

Result (probabilistic method): The approach developed in the methodology chapter has subsequently been applied into analyzing the case study so that its feasibility can be verified.

Discussion: Result obtained from previous sections are presented in this section while some suggestions for further studies are proposed.

Conclusion: Summary of this thesis.

Bibliography: Reference of used publications.

2. Literature review

With the development of geotechnical technology, humanity has the ability to overcome difficulties caused by complicated geological conditions and build various kind of structures on ground and underground. However, there are still some risks remaining known as geohazards, regardless of highly developed technologies (Huang, R. & Li, W.L., 2008). Usually geohazards are caused by geological conditions or human activities, which contribute to the threats to human lives, properties and natural environments. In order to ensure the safety of people with respect to any construction activity, it is important to study and understand how slope stability is assessed and improved.

2.1. Slope stability

2.1.1. General description

Slope failure is one of the most damaging geohazard, and engineers have been trying to find a comprehensive slope stability evaluation system since long time ago (Abramson, L.W., 2002). There are different types of slope failure such as falls, slope slides, toping failure and collapse of the topping retaining structures. Therefore, it is important to study slope stability with respect to safety, economic and environmental requirements.

Usually slopes can be divided into unsupported slopes and supported slopes. Unsupported slopes consist of natural slopes, excavations (cuttings) and loading (embankments). Slopes can also be supported by methods such as soil nailing, sheet pile wall and gravity walls (Fredlund, D.G. & Krahn, J., 1977). Embankments have similar effects on the soil resulting in loading, which leads to change of excess pore pressure and effective stresses in the subsoil. Critical situations may occur if the loading process is too fast. Excavations can also be explained as reloading that decreases the total stress in subsoil. Pore pressure can be reduced during

construction due to temporary drainage while it also increases after construction, so the long-term stability of excavations is also important.

When a slope has an external long surface comparing to other dimensions, it is expected that slide failure happens locally along its surface like shown in Figure 1. (Micro-stability, Barends, F.B., 2011).

According to Phoon, K.K. ed., 2008, safety factor of Micro-slope stability can be explained as in Equation (2.1).

$$Safety\ factor\ (FS) = \frac{(W - ul)\tan\varphi' \cos\beta}{W \sin\beta} = \frac{(\gamma h - \gamma_w h_w)\tan\varphi' \cos\beta}{\gamma h \sin\beta} \quad (2.1)$$

Where
W = weight of sliding material
u = water pressure
l = length of sliding material
β = slope angle
φ' = soil friction angle
γ = unit weight of soil
γ_w = unite weight of water
h = height of sliding material
h_w = height of water level

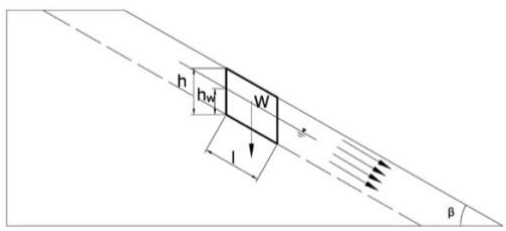

Figure 1: Long slope failure mechanism

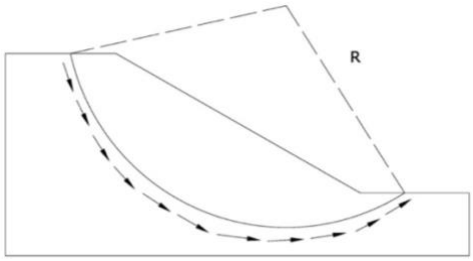

Figure 2: Short slope failure mechanism

On the other hand, a short slope tends to have a circular plastic failure instead of liner failure zone like shown in Figure 2 (Macro-stability, Barends, F.B., 2011; Janbu, N., 1975).

Engineers and scientists have been developing various calculation method for slope stability, e.g. Janbu Method, Bushop's Method and Swedish Slip Circle Method (Janbu, N., 1975; Bishop, A.W.,1955; Hungr, O., 1987; Fredlund, D.G et al., 1981). In Janbu's Method, the slope is divided into several slices and a failure circle is generated for force analysis. Figure 3 illustrates the basic concept of Janbu's Method where the shaded slice is analyzed using force equilibrium. Safety factor of Janbu method is computed as Equation (2.2) (Fredlund, D.G. & Krahn, J., 1977; Janbu, N., 1975).

$$Safety\ Factor\ (FS) = \frac{\sum\{c' l \cos\beta_i + (N - ul)\tan\varphi' \cos\beta_i\}}{\sum N \sin\beta_i + \sum kW_T \pm A - L\cos\omega} \qquad (2.2)$$

Where

c' = soil cohesion

φ' = soil friction angle

β_i = slope angle

l = slice width

u = water pressure

k = seismic coefficient

A = resultant water forces

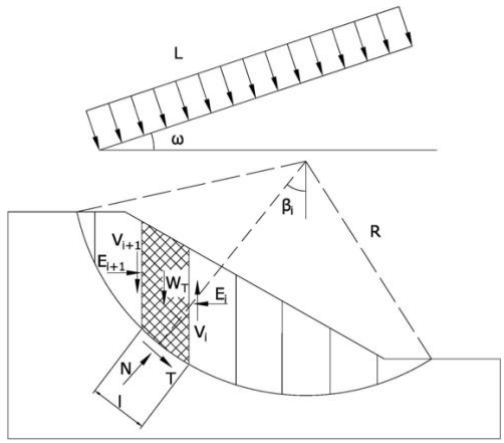

Figure 3: Janbu's method

Slope stability is influenced by soil/rock mass properties and the specific definition of slope failure. Since slope stability is such a major criterion for geotechnical engineering, it should be taken into consideration as one of the important geotechnical risks.

2.2. Calculation and design

Engineers and scientists have been developing different numerical methods to assess the stability of slopes for over centuries. Deterministic methods and probabilistic methods consisting of finite element modeling and inverse computation are presented in this chapter (Abramson, L.W., 2002 & Kliche, C.A., 1999).

2.2.1. Deterministic methods

Deterministic analysis converts input data, like soil properties, load condition and drainage condition etc., into a traditional concept called safety factor by means of mathematical idealization.

2.2.1.1. Limit Equilibrium method

Limit equilibrium is a conventional and well-established approach to analyze slope stability. It investigates the equilibrium between the soil/rock mass and the influence from gravity hence the limit state of the slope will be determined (Davis, R.O. and Selvadurai, A.P., 2005 among others). Based on limit equilibrium theories, many existing calculation methods, e.g. method of slices, Bishop method, Swedish slip circle method and Janbu method, are widely applied.

2.2.1.2. Factor of safety

The conventional method to evaluate slope stability in geotechnical design is to apply a factor of safety. Such factor of safety can be computed from Equation (2.3) (Fenton, G.A. & Griffiths, D.V., 2008 among others).

$$FS = \frac{R}{S} \geq 1 \tag{2.3}$$

where R is the load resistance limit and S is the load effect. This equation has been applied into the industry for many years and it is verified many projects (Abderrahmane, T.H. & Abdelmadjid, B., 2016).

2.2.1.3. Limitation to the deterministic methods

Although the deterministic methods are highly developed and widely applied into industry, it still has shortcomings that the variation of input data is not considered, hence same safety factor may result in different probabilities of failure (Depina, I. et al, 2016). Similarly, higher safety factors do not correlate with higher reliability since the variation is not taken into account (Figure 4) (Lacasse, S., 2016). Sometimes reliability is more important than a single safety factor and deterministic methods could have deviations when used to assess slope stability and probabilistic methods are therefore developed by scientists (Christian, J.T. et al, 1994).

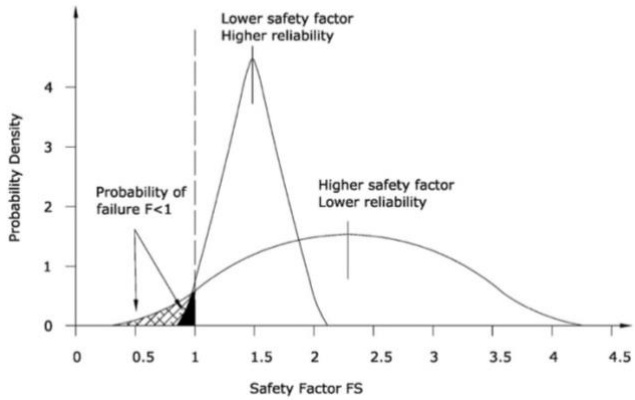

Figure 4: Comparison of safety factor and reliability

2.2.2. Probabilistic methods

Probabilistic analyses consider the soil material uncertainties (variation) and their effects. Griffiths, D.V. el at, 2010 proposed that a probabilistic method needs to obtain its basis from a deterministic method. Given same input data as deterministic method, probabilistic method converts them into probability of failure P_f and reliability index β by means of idealization, including uncertainty. Reliability methods do not eliminate uncertainties but provide a way to organize, qualify and solve them consistently.

Probabilistic tools have reached a mature level in theory and engineers are trying to make them more effective into practices, which could help them understand uncertainties better and focus on safety-cost effectiveness (Cederström, E., 2014).

2.2.2.1. General probabilistic concepts

Assumed that there is a series of variable x that sampled at n points with subscript i. Then the mean value or expected value $E[x]$ ($\mu[x]$) can be calculated from Equation (2.4) (Christian, J.T. et al, 1994).

$$E[x] = \mu[x] = \frac{1}{n}\sum_{i=1}^{n} x_i \tag{2.4}$$

Its variance Var[x] is defined as Equation (2.5).

$$Var[x] = \sigma[x]^2 = \frac{1}{n-1}\sum_{i=1}^{n}(x_i - E[x]^2) \tag{2.5}$$

It can also be calculated from the follow Equation (2.6).

$$Var[x] = E[x^2] - E[x]^2 \tag{2.6}$$

The standard deviation is the square root of variance (Equation 2.7)

$$\sigma[x] = \sqrt{Var[x]} = \sqrt{\frac{1}{n-1}\sum_{i=1}^{n}(x_i - E[x]^2)} \tag{2.7}$$

The coefficient of variation $Cov[x]$ is a dimensionless number that can be computed as Equation (2.8). This equation expresses the standard deviation as a function of expected value. It is particularly used for some variables, like soil strengths and friction angle.

$$Cov[x] = \frac{\sigma[x]}{E[x]} \tag{2.8}$$

The autocovariance of the single variable x over a distance r is computed from Equation (2.9) while the autocorrelation coefficient can be derived from Equation (2.10).

$$C_x(r) = \frac{1}{n-1}\sum(x - E[x]) \cdot (x_{i+r} - E[x]) \tag{2.9}$$

$$R_x(r) = \frac{C_x(r)}{V(x)} \tag{2.10}$$

The Pearson's moment coefficient of skewness measures the asymmetry of the variable x's distribution. It equals the third standardized moment of x (Equation (2.11)).

$$\gamma_1 = E\left[\left(\frac{x - E[x]}{\sigma[x]}\right)^3\right] = \frac{E[x^3] - 3E[x]\sigma[x]^2 - E[x]^3}{\sigma[x]^3} \quad (2.11)$$

If there is another series of a variable y and it is also sampled at n point with subscript i. The covariance of those two variables is expressed as Equation (2.12).

$$C[x, y] = E[(x - E[x]) \cdot (y - E[y])] = \frac{1}{n-1}\sum(x - E[x]) \cdot (y - E[y]) \quad (2.12)$$

The Pearson correlation coefficient $\rho_{x,y}$ between x and y can be obtained from Equation (2.13). This correlation coefficient belongs to an open interval (-1, 1). The closer $\rho_{x,y}$ to 1 or -1, the stronger correlation x and y have. However, Pearson correlation coefficient only applies to linear correlation. Quadratic correlation or other types of correlation rather than linear correlation will not be indicated by Pearson correlation coefficient.

$$\rho_{x,y} = corr(x, y) = \frac{C[x, y]}{\sigma_x \cdot \sigma_y} = \frac{\sum(x - E[x]) \cdot (y - E[y])}{(n-1)\sigma_x \cdot \sigma_y} \quad (2.13)$$

If a safety analysis has been performed and it results in a series of safety factors, its reliability index β can be calculated as Equation (2.14).

$$\beta = \frac{E[F] - 1}{\sigma[F]} \quad (2.14)$$

2.2.2.2. Pointe Estimate method (PEM)

The point estimate method uses a single data calculated from a population parameter to serve as the best estimate of this population parameter. For instance, a sample mean x is the point estimate of the population mean μ_x. Christian, J.T. and Baecher, G.B., 1999 suggested that Rosenblueth's point estimate method generates Gauss-Laguerre quadrature and it can be used to accurately estimate practical programs. Rosenblueth listed three simple but typical cases in his paper (Rosenblueth, E., 1975). Then point estimation method soon became one of the most common method in geotechnical reliability analysis since it is easy to be applied into practice with expectable results.

2.2.2.3.1 Two-point estimation

Assume that X and Y are two random variables and their deterministic relation is $Y = g(X)$. Given the mean value $E[x]$, standard deviation σ_x and skewness coefficient $\mathcal{V}_x$, the approximate expression for the moments of distribution of $g(X)$ can be calculated from Equation (2.15) (Rosenblueth, E., 1975).

$$E[Y^n] \approx P_+ y_+^n + P_- y_-^n \tag{2.15}$$

Where $E[Y^n]$ is the mean value of Y at the power of n. y_+ and y_- are values of Y at point x_+ and x_-. P_+ and P_- are weights coefficient indicating the probabilities that x_+ and x_- occur. Usually x_+ is bigger than $E[x]$ while x_- is less than $E[x]$. When the skewness is zero or neglectable, the distribution of X is symmetric so that x_+ and x_- can be expressed as following Equation (2.16).

$$x_+ = E[x] + \sigma_x \quad x_- = E[x] - \sigma_x \tag{2.16}$$

2.2.2.3.2 N points with a single variable estimation

In the second case where the assumption that skewness is negligible is still applied, Rosenblueth found out that the two variables can be estimated at three or more points. All the points must be symmetric with respect to $E[x]$ due to the symmetry of the distribution. When more point is estimated, higher order approximations can be reached (Rosenblueth, E., 1975).

2.2.2.3.3 More than one variable estimation

There exists a large number of applications of Rosenblueth's point estimation method due to his third case where more than one variable is estimated. In this case, skewness is still zero but different variables might have correlation with each other. Rosenblueth chose 2^n point when there are n variables so that each variable can be estimated at two points, one standard deviation higher or lower than its mean value. Correlation ρ between different variables only affect the weight but not the coordinates. Equation (2.17 2.18) can be applied for estimation when there are n variables.

$$E[Y^m] \approx \sum P_i(y_i)^m \tag{2.17}$$

$$P_{(s_1 s_2 \ldots s_n)} = \frac{1}{2^n}\left(1 + \sum_{i=1}^{n-1}\sum_{j=i+1}^{n}(s_i)(s_j)\,\rho_{ij}\right) \tag{2.18}$$

One generalized case is that Y is a function of three different variables X_1 X_2 X_3 so that there are 8 points to be estimated with different combinations of mean values and standard deviations. As shown in Figure 5, all the 8 points in the coordinate system can be expressed as a cube. The first + or – sign in weight P's subscripts stands for the sign of variable X_1 whether it is estimated at point $E[x_1] + \sigma_{x_1}$ or $E[x_1] - \sigma_{x_1}$(Rosenblueth, E., 1975).

As a result, Equation (2.19-2.22) are summarized for estimation of different weights in cases with three variables. Cases with uncorrelated variable will be easier since the weight will be distributed uniformly for each point.

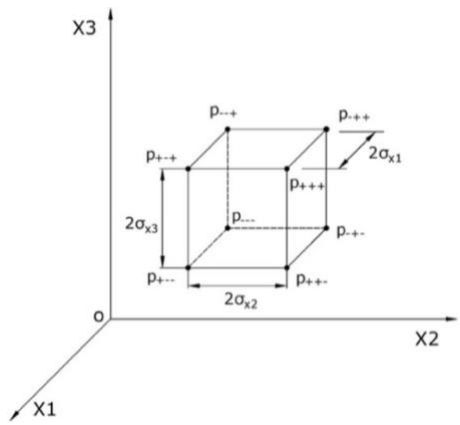

Figure 5: Three variables point estimation

$$P_{+++} = P_{---} = \frac{1}{8}(1 + \rho_{12} + \rho_{23} + \rho_{13}) \tag{2.19}$$

$$P_{+--} = P_{-++} = \frac{1}{8}(1 + \rho_{12} - \rho_{23} - \rho_{13}) \tag{2.20}$$

$$P_{-+-} = P_{+-+} = \frac{1}{8}(1 - \rho_{12} + \rho_{23} - \rho_{13}) \quad (2.21)$$

$$P_{--+} = P_{++-} = \frac{1}{8}(1 - \rho_{12} - \rho_{23} + \rho_{13}) \quad (2.22)$$

2.2.2.3. First Order Second Moment Method (FOSM)

The First Order Second Moment method (FOSM) is commonly applied into uncertainty quantification in geotechnical engineering. Second moment statistics of random variables (mean value and standard deviation) are determined based on the first order Taylor's series expansion at the mean point. The first two moments of random variables X are utilized to compute the second moments of the random response Y (El-Ramly, H. et al, 2002 and Suchomel, R. & Mašın D., 2010).

For instance, the safety factor F can be described by a variate X in Equation (2.23).

$$F = g(X) + e \quad (2.23)$$

If the distribution of X is totally random without any correlation, the variance of the safety factor $Var[F]$ is calculated according to Equation (2.24). Christian, J.T. et al, 1994 successfully utilized FOSM method for uncertainty assessment of slopes.

$$Var[F] \approx \sum_{i=1}^{k} \left(\frac{\partial g}{\partial x_i}\right)^2 V[x_i] + V[e] \quad (2.24)$$

2.2.2.4. First Order Reliability Method (FORM)

Based on FOSM, the First Order Reliability Method (FORM) focuses on a design point of the first order Taylor's series where the failure limit with the highest value of probability density function. It corresponds to the point on failure limit closest to the origin among all the random variable.

The FORM method has overcome several drawbacks that FOSM method cannot solve. The reliability index is independent from the

performance function. However, the accuracy of FORM gets lower when the performance function is nonlinear.

2.2.2.5. Second Order Reliability Method (SORM)

The Second Order Reliability Method (SORM) uses the second order approximation of the performance function at the design point. Generally, it provides better accuracy than FORM but consumes more calculation or time (Der Kiureghian. A., 2005).

2.2.2.6. Monte Carlo Simulation (MCS)

Monte Carlo Simulation (MCS) functions by repeating random sampling to predict the result. It repeats the procedure of performing each random variably many times so that a sample probability distribution will be obtained as an outcome. Monte Carlo Simulation is an explicit probabilistic framework. El-Ramly, H. et al, 2002 have developed a spreadsheet approach for slope stability by combining MSC and numerical software together for slope stability assessment.

Monte Carlo Simulation has solved the problem caused by nonlinearity and it gives accurate estimation of failure probability (Wang, Y., Cao, Z. & Au, S.K., 2010). Additionally, MCS method cooperates well with other deterministic tools (Davis, T.J. & Keller, C.P., 1997). However, it takes large number of samples and time to perform such a simulation and it is insufficient when a complicated model is used.

2.2.3. Finite element modelling

With the development of PC as well as software technology, finite element modelling has been increasingly used in slope stability assessment (Matsui, T. and San, K.C., 1992). It gives estimations of stress, strain and some other properties of a slope. There are two major approaches to assess slope stability in finite element modelling, either increasing external loads or reducing the strength parameters of soil mass (Griffiths, D.V. & Lane, P.A., 1999).

Various finite element programs have been developed by engineers to deal with different kinds of complex geotechnical problems. A brief summary of other researchers' work is shown in Table 1.

2.2.3.1. Random finite element method (RFEM)

Random finite element method (RFEM) is a powerful slope stability analysis tool that fully accounts for spatial correlation and averaging based on traditional finite element method. One advantage is that it does not require a priori assumptions on the shape or the location of the failure mechanism. Griffiths, D.V. et al, 2005 proved the feasibility of RFEM by applying it into the slope stability assessment of an undrained slope.

Table 1 Summary of FEM programs

Reference	Problem	Program
François, B. et al, 2006.	Mechanical behavior of a large slope movement	Z_Soil and Feflow
Islam, M.R. & Faruque, M.O., 2012.	Rock strength factor and tension zones near an overall pit slope	Phase2
Sanavia, L., 2009.	Slope stability regarding water pressure variation	GiD
Fawaz, A. et al, 2014.	Mechanical parameters of soil layers constituting the slope	Plaxis
Moni, M.M. & Sazzad, M.M., 2015.	The response of a slope with strength reduction	GEO5
Pham, H.T. & Fredlund, D.G., 2003.	Slope stability	DYNPROG

2.2.3.2. Strength reduction methods

The traditional approach to decide the safety factor is to increase the load incrementally until failure so that the difference between failure load and actual load is studied (Griffiths, D.V. & Lane, P.A., 1999). But sometimes

in practical work, strength reduction methods will be applied as alternatives (Dawson, E.M. et al, 1999).

One procedure is called $\varphi - c$ reduction method. The strength parameters (c, phi) are gradually reduced until failure while keeping load constant instead of changing it. In some finite element programs like Plaxis, the Mohr-Coulomb failure surface is lowered incrementally and the cohesion a is kept constant until large deformations appear. A new form of safety factor, multiplier for safety factor MSF, is then defined as the ratio between actual strength and reduced strength (Steinar N., 2017). As shown in Figure 6 and Equation (2.25), the calculation will be continued until it reaches a well-developed plastic failure and a well-defined safety factor.

$$MFS = FS = \frac{tan\,\phi}{tan\,\rho} \tag{2.25}$$

Apart from phi-c reduction, there is a second strength reduction method called gravity increase method (GIM) according to Abderrahmane, T.H. & Abdelmadjid, B The gravity force in this case, or weight, is increased until the failure of the slope. See Equation (2.26).

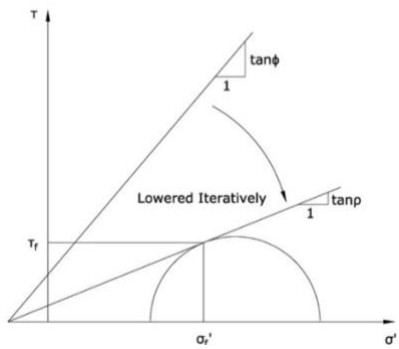

Figure 6: Phi-c reduction

$$FS = \frac{g_0^{trail}}{g_0} \tag{2.26}$$

2.2.4. Inverse calculation

Sometimes when measurement data and numerical analysis are both available, inverse calculation can be performed to minimize the error between numerically computed result and in-situ measurement, which can then calibrate models that has been already used (Calvello, M. & Cascini, L., 2006). They also proposed a new model called R-u-F-v prediction model including inverse calculation.

Inverse methods include direct and indirect methods. But mostly people will choose indirect methods like Bayesian method, Kalman filter (KF) or maximum like-hood methods (Vardon, P.J. et al, 2013; Sah, N.K. et al, 1994). All those inverse methods are capable to interact with other models. Hsiao, E.C. et al, 2008. applied inverse calculation into KJHH model, a semi-empirical model, to assess the serviceability of buildings.

Inverse calculation is also widely used for adjusting and optimizing constitutive soil models. Vahdati, P. et al, 2013. combined inverse calculation with genetic algorithm and successfully analyzed soil parameters of a rockfill dam while Papon, A. et al, 2012. optimized two different constitutive soil models by performing inverse analysis.

Therefore, inverse calculation is a feasible approach to optimize existing numerical models in order to reach better results.

2.3. Field measurement

Due to safety and environment requirements, field measurements are often performed to monitor the deformation of slopes. Monitoring is usually achieved by utilizing instrumentation that consists of two major categories. The first type of instrumentation is used for in-situ determination of soil/rock mass properties during the design phase while the second type is mainly used for performance monitoring during the construction or operation phases (Dunnicliff, J., 1993).

For slope stability, people usually focus on its deformation both on and beneath the surface, hydrological conditions and pore pressure (Millis, S.W. et al, 2008). There aspects are the basis of a field measurement system.

2.3.1. Deformation measurement

Among the methods to determine whether a slope faces its failure or not is to monitor its deformation since large plastic deformation is a sign of slope failure (Davis, R.O. and Selvadurai, A.P., 2005).

2.3.1.1. Inclinometers

Inclinometers are widely used for measuring subsurface deformation, even the direction and magnitude of slope movements. As a result, it is an effective way to use inclinometers to study the cause, development and behavior of slope failures (Stark, T.D. & Choi, H., 2008). Inclinometers can be divided into two categories, portable inclinometers and in-plane inclinometers (DGSI. Durham Geo Slope Indicator, 2017). In-plane inclinometers generate more data than portable inclinometers and usually those data will be processed and distributed immediately by the monitoring system (Millis, S.W. et al, 2008).

An inclinometer system has two components, an inclinometer measurement sensor and a casing (mostly made of plastic or fiberglass). A flexible casing is important when people want to detect small amount of movements (Stark, T.D. & Choi, H., 2008). Casing should be paid more attention since its contact with soil influences the in-plane inclinometers' orientation, depth and position, which might result in unexpected errors (Salewich, C., 2012; DGSI. Durham Geo Slope Indicator, 2017).

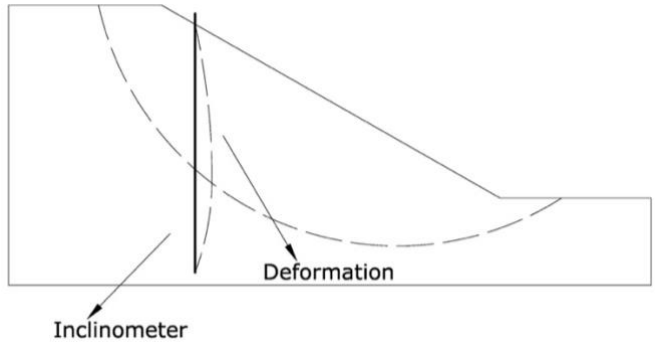

Figure 7: Inclinometer installation

Usually inclinometers are installed in a borehole, but they are also possible to be embedded in fill, casted into concrete or attached to a structure (DGSI. Durham Geo Slope Indicator, 2017). All the inclinometers have to be installed into the subsurface and preferable deeper than the theoretical yield circle (Figure 7). In fact, the accuracy of measurement depends on the quality of inclinometer installation as well (Machan, G. & Bennett, V.G., 2008).

2.3.1.2. Other instrumentation

Time-domain reflectometry (TDR) is an alternative measurement technique that observes slope movements by means of reflected waveforms. In 1980, TDR was first used as a geotechnical tool to discover shear zones in a coal mine (Wade, L.V. & Conroy, P.J.,1980). TDR is also verified to be sensitive to concentrated shear strains so that it can collaborate well with inclinometers (Dowding, C.H. & O'Connor, K.M., 2000; Kane, W.F. & Beck, T.J., 2000).

2.3.2. Porewater measurement

Porewater pressure is another important criterion of slope stability monitoring (Dunnicliff, J., 1993). The most common instrument to monitor porewater pressure is Piezometer that measures both porewater pressure and ground water pressure at the same time. Alternatively,

observation wells and tensionmeters can also be chosen (Damiano, E. et al, 2012).

According to DGSI. Durham Geo Slope Indicator, 2017, there are four major types of piezometers. Standpipe piezometer is the basic type whereas Vibrating Wire Piezometer is the most deployed type (Salewich, C., 2012; Kane, W.F. & Beck, T.J., 2000). Pneumatic Piezometer functions by gas pressure and Titanium Piezometer is designed for drawdown tests.

The installation of piezometers is as significant as inclinometers. Simoni, A. et al, 2004. have come up with an alternative method utilizing piezometers with piezoresistive bridges, which responds faster to porewater pressure variations compared to usual installation. Huang, A.B. et al, 2012 developed a piezometer system based on optical Fiber Bragg Grating (FBG) pressure sensors.

2.3.3. Database system

To analyze complicated and large quantities of measurement data more productively, it is essential to create suitable database systems for better management. A successful and feasible database system should combine remote sensing techniques and electronic measurement instrumentation, together with an alarm system to notify people when slope failure occurs (Kane, W.F. & Beck, T.J., 2000; Vanneschi, C, 2017).

There are already plenty of database systems in the market like the real-time slope monitoring system adopted by Geotechnical Engineering Office (GEO) of the Government of the Hong Kong SAR (Millis, S.W. et al, 2008). More investments should be made for better and more powerful database systems in the future.

2.4. Risk analysis

The definition of risk varies with different views (Fenton, G.A. & Griffiths, D.V., 2008). It can be expected loss or probability of an undesired event. It is defined as effect of uncertainties on objectives with a minor adjustment, only negative effects are considered (ISO 31000:2009, 2009). It can be also defined as the product of consequences and the probably of failure (Baecher, G.B. & Christian, J.T., 2005). Before building up a risk analysis system, it is necessary to study the geotechnical uncertainties.

2.4.1. Uncertainties

Geotechnical uncertainties not only include geological conditions but also uncertainties within technical, contractual and operational aspects (Spross, J. et al., 2015). There are two major types of geological uncertainties in general.

Aleatoric uncertainty is related to natural variability of the system. It cannot be reduced by conducting more observations, but it can be better described. On the other hand, epistemic uncertainty is caused by incomplete knowledge and it can be reduced by repeating observations. For example, the contractor tries to perform enough site pre-investigation (Drilling, mapping etc.) in order to find out the weakness zone or fracture on site. In this case, uncertainties due to insufficient investigation will be reduced. There are also other epistemic uncertainties including statistical errors and transformation errors, like those shown in Figure 8.

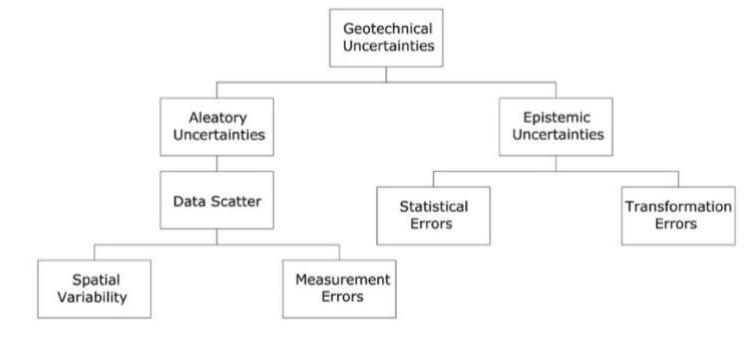

Figure 8: Geotechnical uncertainties (Spross, J. et al., 2015)

To deal with these uncertainties and provide a better contractual environment, it is necessary to develop a sort of risk management system as a basis of project management. A complete risk management system should consider both structural safety and environment safety while project economy and third-party disturbance should also be paid attention on (Spross, J. et al., 2015).

A good risk management system should not only focus on structural or geotechnical aspects but also other on threats against the project, including feasibility, tendering, design, construction and operation (Fenton, G.A. & Griffiths, D.V., 2008). Respect and full cooperation between each party are also required (Norwegian Tunneling Society NFF, 2012). Dai, F.C. et al, 2002 has developed a risk analysis framework for landslides by assessing the probability of landslide failure and vulnerability. Thus, risk management is quite important with respect to safety and economy.

3. Methodology

In this chapter, a simplified methodology for slope stability assessment is developed. It is centered on uncertainties within geotechnical ground conditions such as soil parameters and dimensions of the constructed structures. The proposed probabilistic methodology makes the stability analysis more transparent and objective than subjective deterministic methods. This methodology is tested on Nya Slussen project in the following chapter.

3.1. General inverse analysis

Inverse analysis is an idea that the simulated result from a numerical model is compared and updated with the measurement data in reality. Properties estimated from inverse analysis can be used as a new initial value into forward calculations. Inverse analysis calibrates a numerical model with respect to the field measurement so that the uncertainties in the model can be reduced (Figure 9).

Generally, there are two types of inverse analysis methods, direct and indirect methods. They are classified according to the relationship between input model parameters and field measured data.

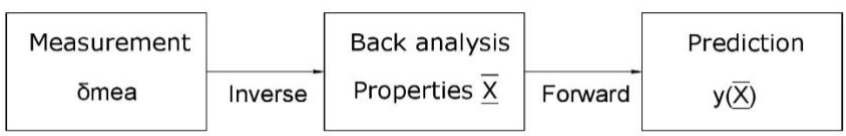

Figure 9: Inverse analysis

3.1.1. Linear inverse analysis

When linear relationships exist between modelled parameters and filed measured data, direct methods are suitable to be used (Vardon, P.J. et al, 2016). Those parameters are estimated directly by applying the linear equation on data. For instance, a linear deformation is modelled for an elastic material with Young's modulus E. Its stress $\Delta\sigma$ and deformation ΔH are measured throughout the whole loading process (Figure 10). The elastic linear relationship between E, $\Delta\sigma$ and ΔH can subsequently be derived. E is simply calculated as the ratio between measured stress and strain (Equation 3.1) in inverse analysis and then the obtained value of Young's modulus can be used for further calculation.

$$E = \frac{\Delta\sigma}{\varepsilon} = \frac{\Delta\sigma}{\frac{\Delta H}{H}} \tag{3.1}$$

If there is a single parameter that needs to be estimated, the methodology could follow the example presented above. A linear equation is established, and the parameter is calculated from this equation. Suppose that there are more than one parameter existing in the model, it will become more complicated to use just one single formula.

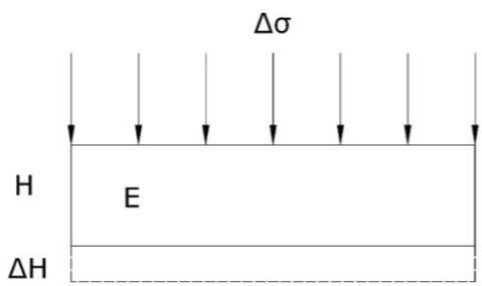

Figure 10: Direct method

3.1.2. Non-linear inverse analysis

Indirect methods are applied to those nonlinear and non-uniqueness relationships between modelled parameters and data (Calvello, M. & Finno, R.J., 2004). If a nonlinear plastic relationship exists in the example made for direct method, then it is cumbersome to derive a deterministic equation for this case. Therefore, an alternative way is developed by minimizing the absolute difference between measured data and calculated data to find the nearly perfect estimated values for parameters (Honjo, Y et al, 1994).

Indirect methods are more suitable since perfect linear relationships typically do not exist in nature. For the calculations finite element model can be used. Significant difficulty is to couple the modelled and the measured by repeating running the model with different input data. Sometimes it could be time consuming so that some simplifications and assumptions can be proposed.

To summarize, inverse analysis is a feasible approach to assess the slope stability during construction since the chosen parameters can be calibrated with measurements (Zentar, R.H.P.Y. et al, 2001). Direct methods suit better with easier cases where only linear relationships exist while indirect method can be utilized widely in geotechnical engineering due to its flexibility (Bin, C. et al, 2004). Indirect methods are hence used this slope stability assessment system.

3.2. Simplified inverse method

3.2.1. Flowchart of the systemic method

The flowchart in Figure 11 gives the general description and procedures of the methodology of the slope stability assessment system. The system is divided into three parts: deterministic design, inverse analysis and forward calculation. Inverse analysis is the primary structure in this system since probabilistic methods are used to decrease the uncertainties from

deterministic design. A new factor of safety is calculated from forward analysis as the improved estimation of slope stability.

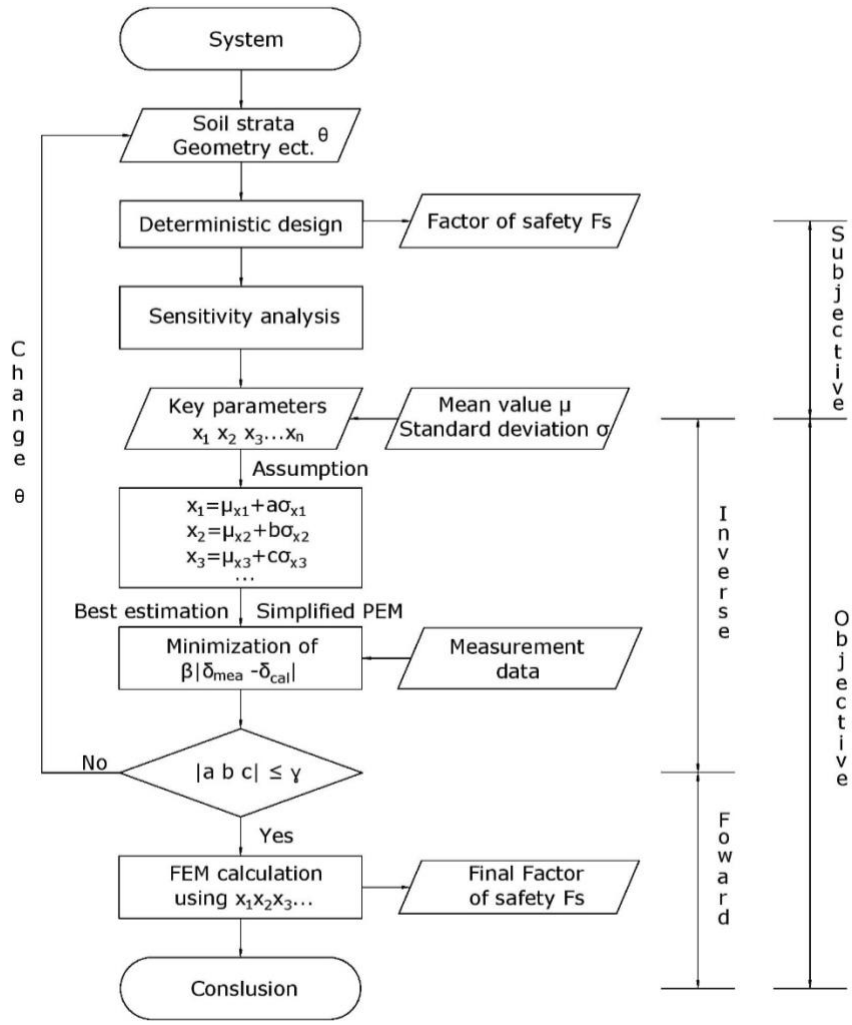

Figure 11: Flowchart of the slope stability assessment methodology

3.2.2. Deterministic design

As mentioned in the literature survey, deterministic design is the most popular and widely used method in the industry (Whitman, R.V., 2000). Usually a finite element model is built in deterministic design phase if a complicated construction activity needs to be checked with its safety requirements.

In this system, it is suggested to use Plaxis 2D as the finite element tool throughout the whole procedure. All the input data like geometry or soil parameters are taken direct from pre-construction investigation. For some important soil parameters with great uncertainties, conventional values or empirical values are used instead of the soil data from geotechnical investigations.

A factor of safety (FS) is calculated from Plaxis 2D after deterministic simulation. However, there are still uncertainties remaining. Thus, it is necessary to conduct probabilistic analysis in this methodology.

3.2.3. Sensitivity analysis

Sensitivity analysis is a mathematical approach where uncertainties can be minimized by testing different input data into an existing model. For example, in a finite element model, the tested parameters can be geometrical entities or soil properties, even external load and time. The selection of tested parameters can vary depending on different prerequisites (Cao, M. & Qiao, P., 2008).

When a certain parameter is under simulation in the models, it is important that the other parameters stay constant so that they will not affect the output result, which is known as the One-at-a-time rule. Some secondary parameters might be neglected if they show less impact on the total stability. For those parameters that have a significant influence on total stability in the model, they can be processed into further steps.

The benefit of sensitivity analyses is that a clear connection between different parameters and slope stability are created. An overview of uncertainty distribution is obtained. Although it requires repetition of running the same model with just one change in a parameter each time, it is still a powerful tool as a preliminary design tool in the probabilistic design phase since it screens out the parameters with most uncertainties.

3.2.4. Main procedure

First of all, it is important to choose a main criterion for an inverse analysis since it is an indirect analysis. It might be displacement at different directions, pore pressure or soil stresses etc. In this thesis, displacement is used as the main criterion for the system of slope stability assessment. The purpose is to minimize the difference between simulated displacement and field measured displacement with respect to different input model parameters. Equation 3.2 is derived from indirect Bayesian formulation according to Honjo, Y et al, 1994.

$$min\, D_0(\theta) = min \sum_{i=1}^{n} \beta_i \cdot \Delta\delta(x_i|\theta) = min \sum_{i=1}^{n} \beta_i \cdot |\delta_{mea}(t) - \delta_{cal}(x_i|\theta)| \quad (3.2)$$

where θ is the model parameter such as model geometry and drainage conditions. x_i is the input variables regarding soil properties that needs to be tested while β_i is the corresponding factor that adjusts the significance of the variables x_i. δ_{mea} and δ_{cal} stand for the measured displacement and calculated displacement respectively. The idea is to find the proper values of variables x_i so that the sum of difference between the measured and the modelled is minimized.

This equation is a simplified version derived from the extended Bayesian method (EBM) where the extra subject information is considered. With only the object information it is called the least square method (LSM). LSM provides great simplicity and convenience because no prior information is introduced, and it is assumed that all the observation values have the equal weight. However, weight from different components is introduced with a weight factor β_i $(0 < \beta_i < 1)$. It hence becomes the

maximum likelihood (MLM) or the weighted least square method (WLSM).

3.2.5. Simplified point estimate method and iteration

After the key parameter and main formula have been determined, it is necessary to figure out a suitable probabilistic approach to conduct the main formula into practice. However, most of them are too complicated and unpractical in the current study. For example, Monte Carlo Method (MCM) is a feasible way to achieve considerable results by repeating the same finite element model many times, but it consumes too much time. Instead, a simplified approach inspired by Point Estimation Method (PEM) is developed in this project.

Assume that there is a series of main parameters $x_1 \cdots x_n$ and their mean values μ_{x_i} and standard deviations σ_{x_i} are known from pre-construction investigations. The purpose is to find the values of those key parameters that provide results as similar as field measurement through finite element modelling. Inspired by the third case in Rosenblueth's paper of point estimation, the model will be run 2^n times to estimate the expected output criterion like displacement or stress (Rosenblueth, E., 1975). Each parameter must be estimated at two points ($\mu_{x_i}+ \sigma_{x_i}$ and $\mu_{x_i}- \sigma_{x_i}$) so that it becomes 2^n combinations of n parameters. If part of inverse analysis does not correspond to the measurement so well, or if there is something irrational with the measurement data, its weight factor β_i is set at a lower value, otherwise it is set according to the past experience or 1. This step gives a rough estimation of the expected criterion and guideline for the following calculation steps.

After the point estimation, each parameter is assigned with a factor $(a, b, c \dots)$ so it becomes $x_i = \mu_{x_i} + (a \; or \; b \; or \; c \dots)\sigma_{x_i}$. Then the optimization method is performed to find the best estimation of those factors with respect to the minimization in Equation 3.2.

To control those factors $(a, b, c \ldots)$ in a reasonable range, a limit value γ is created manually. If the absolute values of those factors are more than the limit value, the geometry and soil parameters should be changed. Assume that normal distribution is hypothesized to all the parameters, there is only 5% possibilities that values will fall out of the interval of $\mu_{x_i} \pm 2\sigma_{x_i}$. The model should be modified, and the simulation is continued as an iteration until a best estimation that fulfills the requirement has been found.

3.2.6. Forward calculation

When the modelled and the measured criterion correspond to each other, all the values of those key parameters are ready to be used in the forward calculation. The process is straightforward in forward calculation since uncertainties are already lowered by inverse analysis. After all the key parameters are determined with their best optimized values, the model is run for the last time to provide a final factor of safety FS_{final}.

4. Case study: the Nya Slussen project

In this chapter, a case study concerning slope stability at the Nya Slussen project located in central Stockholm is presented. Four cross sections of a slope between the excavation and the existing metro line are analyzed.

4.1. Background

Slussen was completed on 15 October 1935 by Architect Tage William-Olsson and Engineer Gösta Lundborg as the first cloverleaf interchange for inner-city traffic in Europe. It connects Gamla Stan and Södermalm, which has been offering convenience for transportation since then (Stockholms Stad, 2017).

However, after 70 years of usage, several accidents have occurred due to concrete aging or weathering, such as concrete fall and concrete fractures (Strålin, J., 2007). The southeast part of Slussen has been facing with ground settlements because of inadequate piling. The traffic demand is also increasing (ELU Konsult AB, 2017). Therefore, Slussen requires a complete reconstruction.

The initial idea of Nya Slussen was brought up in 2004 by Stockholm Stad (The city of Stockholm) together with several architecture firms and engineering consultant companies. The plan intends to ensure that Nya Slussen not only functions as a transit terminal for different kinds of transportations but also as a cultural center for people to visit. The construction area starts from Peter Myndes Backe to Stockholm inflow, including some parts of Gamla Stan (Figure 12). The construction of the new main bridge's foundation has begun in 2017 (ELU Konsult AB, 2017).

s

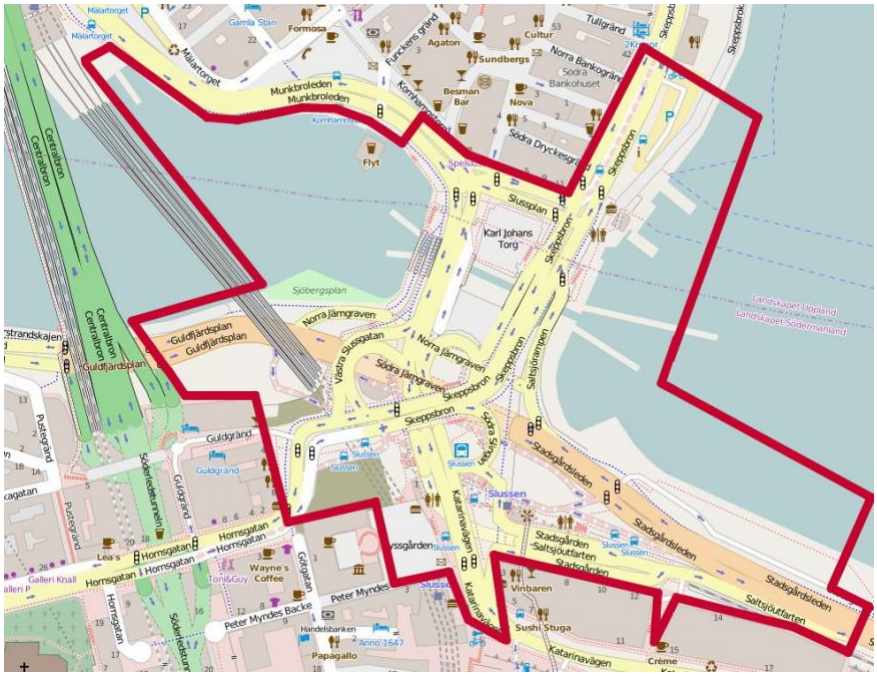

Figure 12: Planned Nya Slussen (Stockholms Stad, 2017)

Since the reconstruction of Nya Slussen is carried out in the city center where people live and work every day, the safety class is set to SK3 (Säkerhetsklass 3) according to SS_EN 1990 (Karlsson, M. & Moritz, L., 2014). This project involves many complicated geotechnical and geological problems where intensive monitoring and risk assessment must be performed during the whole construction process. Any consequence like settlements, vibrations and noise, are necessary to be considered. (Stockholms Stad, 2017).

This thesis mainly focuses on four different cross sections of Slopes R1 near the existing metro red line. Details of those slopes are presented in the next subchapter.

4.2. Location and geometry

4.2.1. Location

As mentioned before, Nya Slussen project is located between Södermalm and Gamla Stan, Stockholm whereas Slope R1 lies in the south of this reconstruction zone. The geographical coordinates of Slope R1 is approximately 59°19'11.9"N, 18°04'20.2"E and it is oriented nearly north-north west (NNW) to south-south east (SSE). As shown in Figure 13, Slope R1 lies just next to the Slussen metro station and Katarinavägen hence its stability is undoubtedly significant with respect to public safety. Metro lines usually have higher sensitive levels for safety because even small displacements can cause serious consequences.

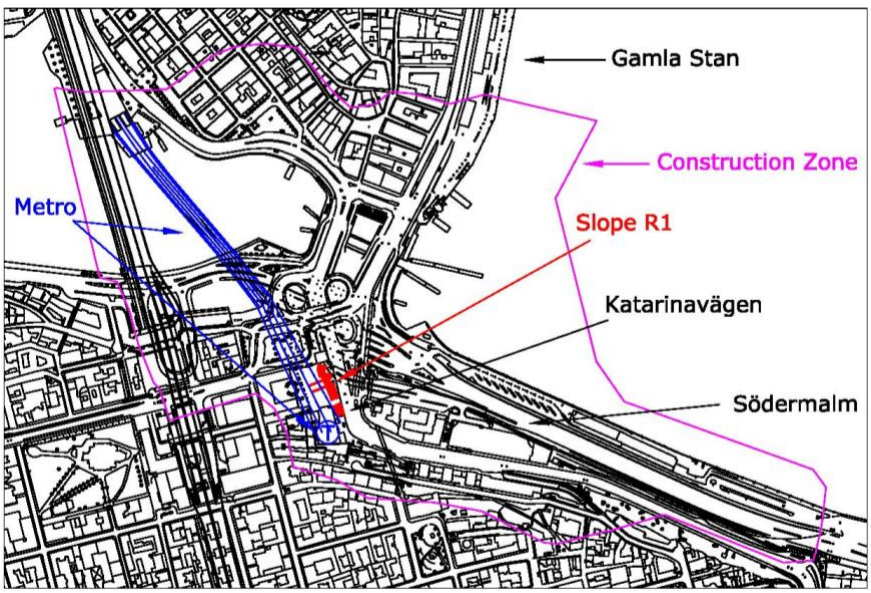

Figure 13:Location of Slope R1

4.2.2. Cross sections (CS)

Figure 14: Locations of cross sections

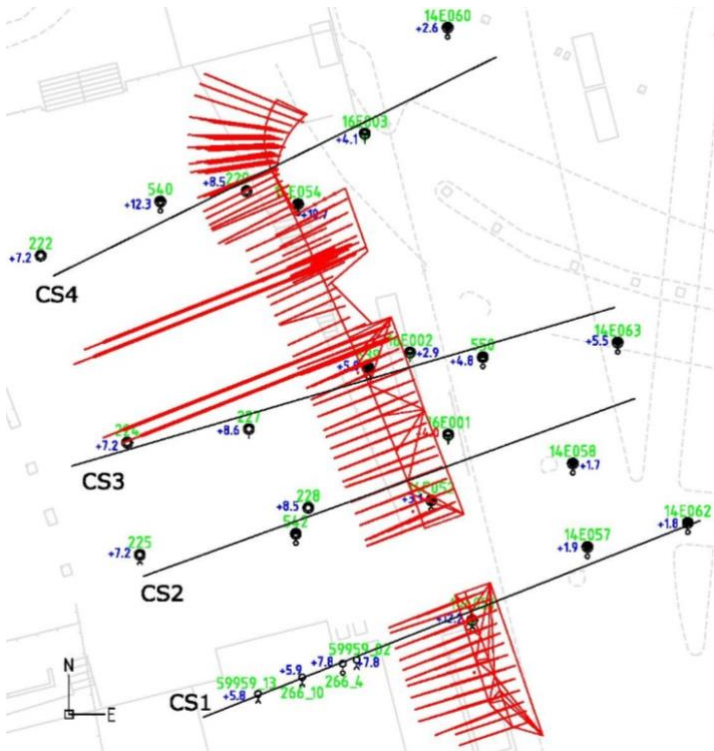

Figure 15: Top view of cross sections and boreholes of Slope R1

There are four cross sections in Slope R1 that are analyzed in this thesis. Figure 14 shows the real site situation of those cross sections where CS1, CS2, CS3 and CS4 are located sequentially from the south to the north of Slope R1.

All the cross sections were chosen to represent different parts of Slope R1. There is a tunnel between CS1 and CS2 while CS3 and CS4 are separated by a sheet pile wall. Details are presented in Figure 15.

4.2.2.1. CS1

CS1 represents the part of Slope R1 that starts from the south end of it to the passageway. The footing of the existing metro's foundation is assumed to be at the same level as ground level, which is +3.55 m in this case. The upper edge of the slope is 1 m away from the foundation footing. The slope consists of two parts with different angles where reinforced shotcrete and soil nailing were installed to ensure the stability. Shotcrete is applied all over the slope surface while soil nails are installed at different levels (+0.7 m, +1.3 m, +2.55 m and +3.55 m). Excavation was made until the foot of the slope at level 0 m. (Figure 16).

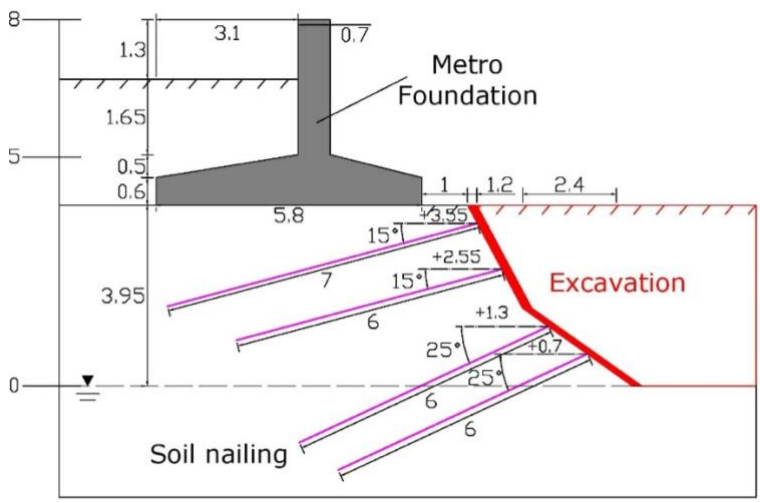

Figure 16: Details of CS1

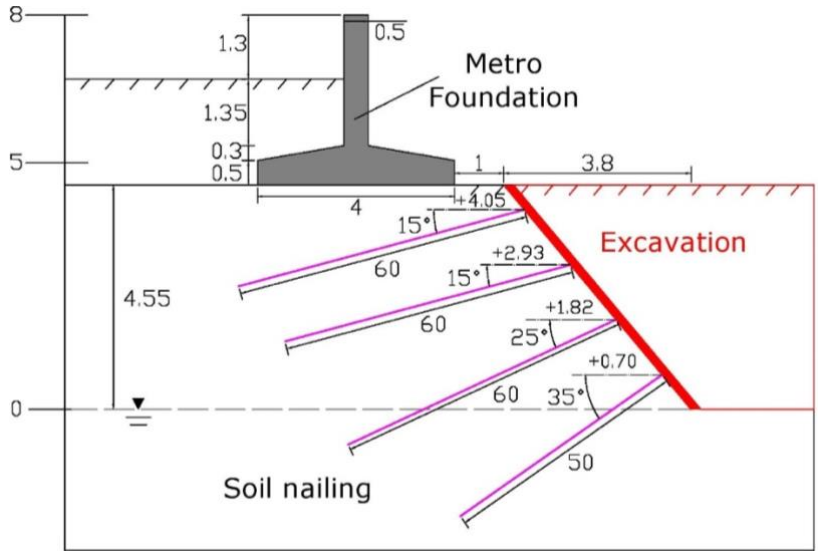

Figure 17: Details of CS2 and CS3

4.2.2.2. CS2 and CS3

CS2 and CS3 represent the middle part of Slope R1 between the passageway and the sheet pile wall. The ground level is located at 4.55 m together with the level of the foot of existing metro's foundation. The distance between the existing foundation and the slope is also 1 m. The slope is a single slope with only one angle where shotcrete and soil nailing are applied. Reinforced shotcrete covers the whole slope and soil nails are installed at +0.7 m, +1.82 m, +2.93 m and +4.05 m, respectively (Figure 17).

4.2.2.3. CS4

As the last part of Slope R1, CS4 is slightly different from other cross sections because the first part of the slope is quite steep, nearly vertical. The level of its upper edge is also 4.55 m same as ground level, while it locates 1 m away from the existing metro's foundation. Shotcrete is applied for CS4 but only three levels of soil nails are installed in this case at +2.75 m, +3.4 m and +4.05 m (Figure 18).

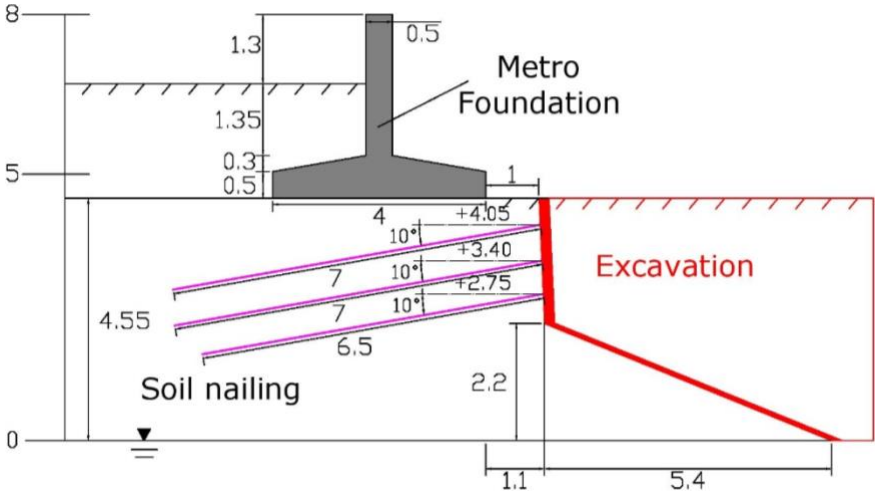

Figure 18: Details of CS4

4.3. Geotechnical/Geological conditions

The geotechnical/Geological conditions are the most important part of pre-investigation since they provide a brief estimation of uncertainties related to the construction activities. In the Nya Slussen project, intensive core-drilling, probe-drilling, CPT testing and laboratory testing were performed to investigate ground conditions. The geological conditions near those cross sections are presented in this part.

4.3.1. Soil layers

The ground conditions near Slope R1 are summarized into four charts for each cross section based on the ground investigation data. The red parts stand for excavation boundaries while purple lines represent soil nails installed to stabilize Slope R1.

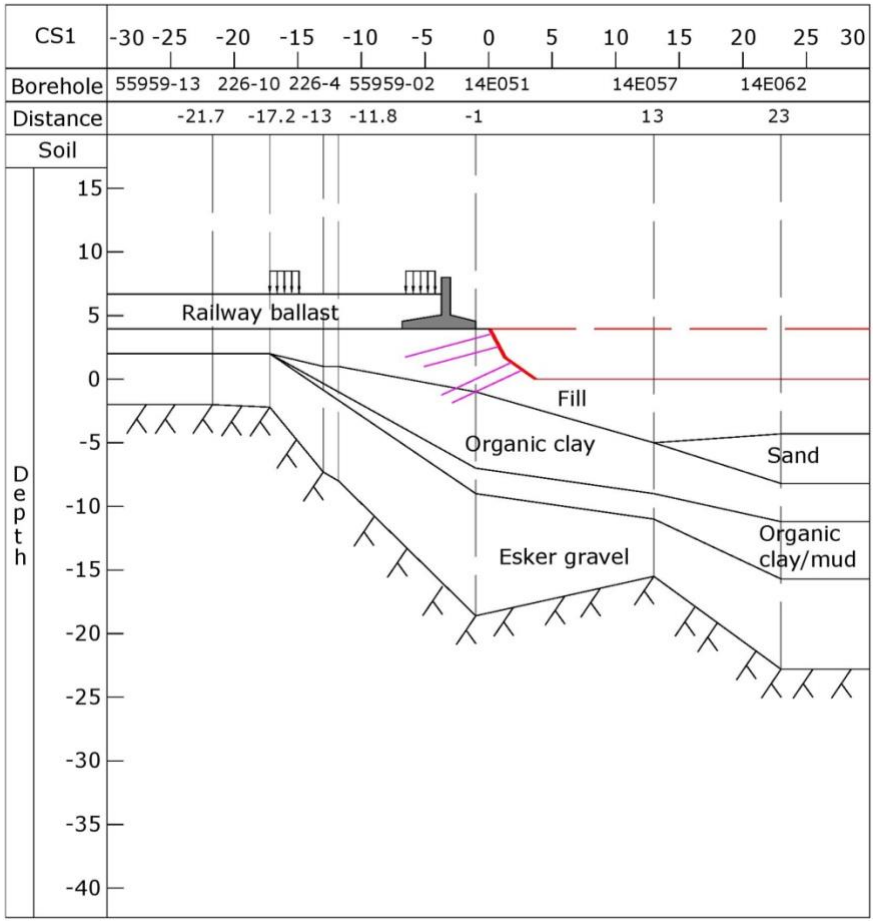

Figure 19: Soil profile of CS1

4.3.1.1. CS1

As shown in Figure 19, the bedrock is very close to ground level near the west side of CS1 while it descends deeper near the east side. There are two organic clay layers and one sand layer between the fill and gravelly soil. Excavation activity were carried out within the distribution range of fill, but the stability of organic clay still needed to be checked.

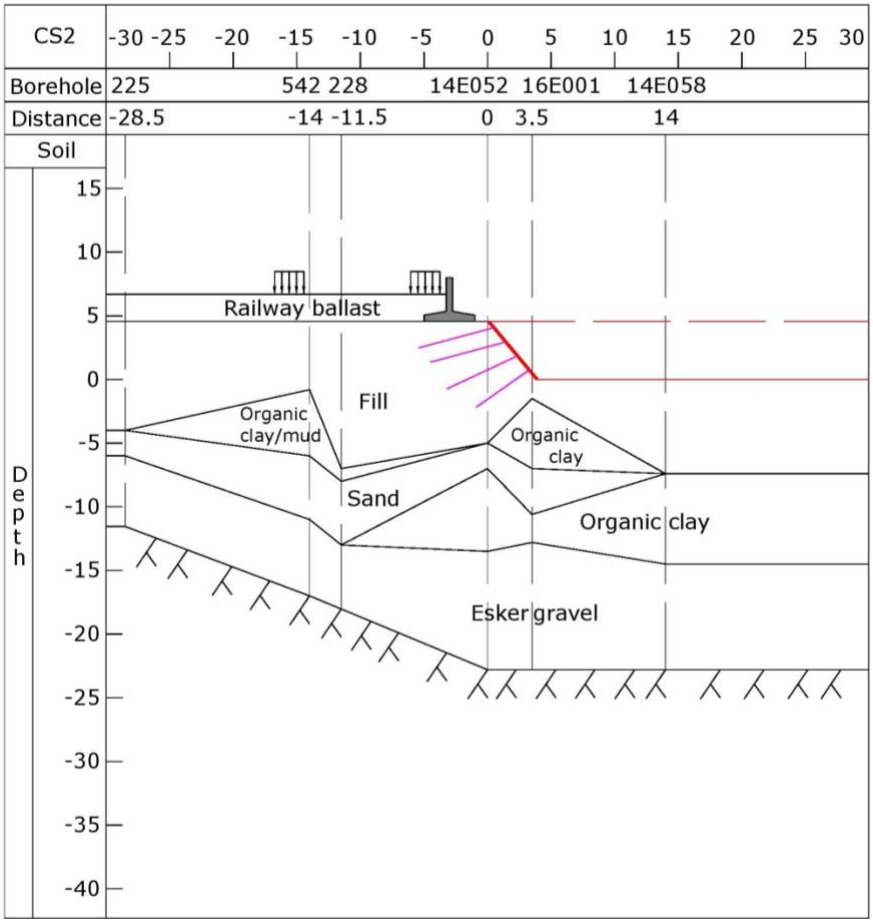

Figure 20: Soil profile of CS2

4.3.1.1. CS2

From Figure 20, the ground conditions under CS2 are quite different from CS1. There are two types of mud underneath the slope, organic clay and organic clay/mud. Organic clay/mud exists in the west of CS2 whereas organic clay takes up most of the space in the east of CS2 between filling and gravel soil. Additionally, the excavation activities almost reached one of the organic clay layers.

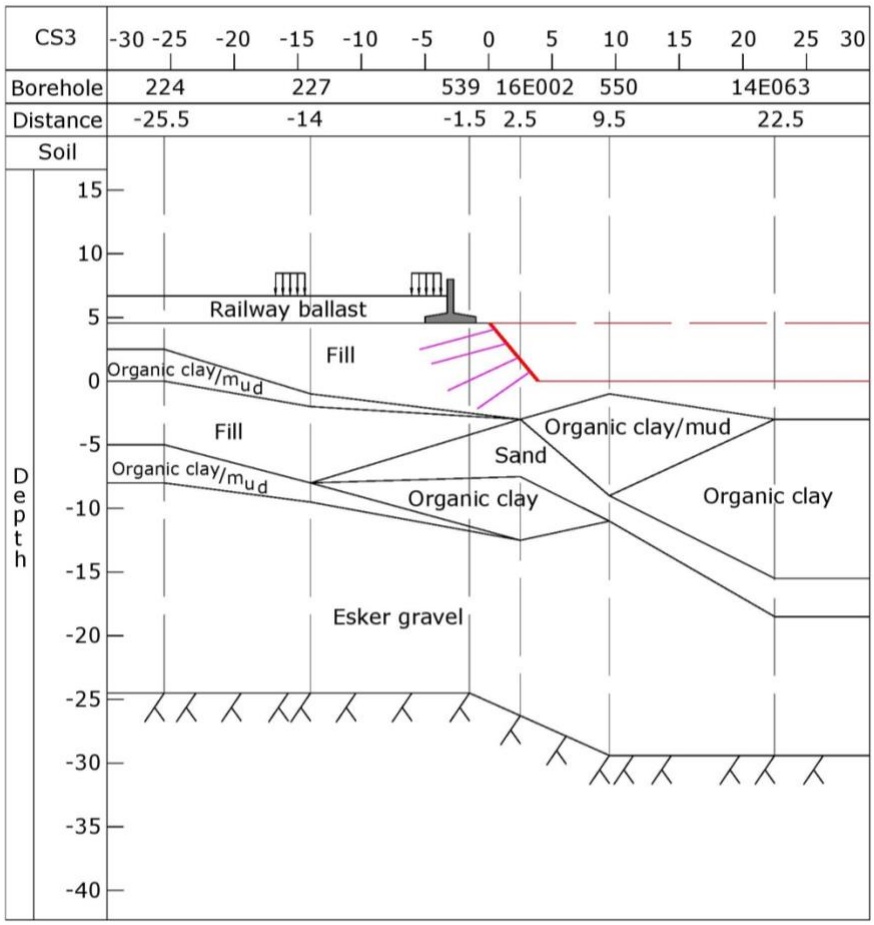

Figure 21: Soil profile of CS3

4.3.1.1. CS3

The soil distribution under CS3 is more complicate than other cross sections since all types of soil mix with each other. Also, the level of bed rock is flatter and lower than the previous cross sections (Figure 21).

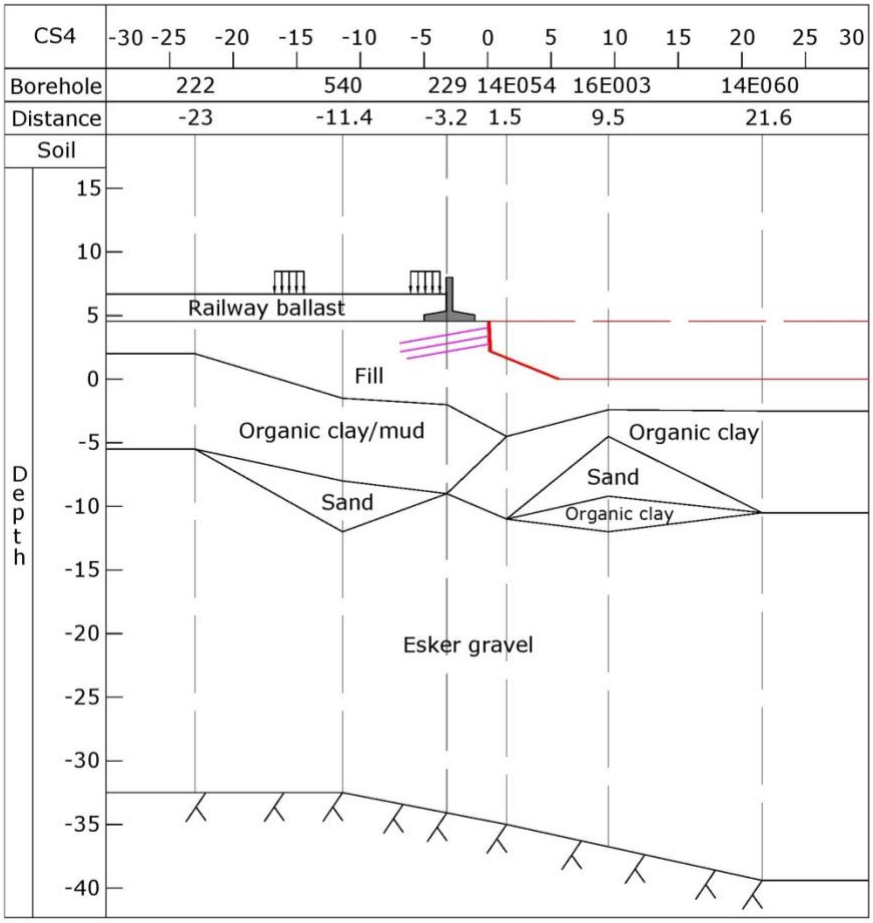

Figure 22: Soil profile of CS4

4.3.1.1. CS4

Figure 22 shows that the soil distribution under CS4 is similar to CS1 where organic clay/mud locates in the west of R1 and organic clay lies in the east. The bed rock level is also deeper than other cross sections. Excavation were only carried out within the filling.

4.3.2. Soil parameters

Soil parameters are obtained from CPT tests during pre-construction investigation for each type of soil. Since great uncertainties exist regarding the soil parameters, significant assumptions were proposed in the case study.

4.3.2.1. Fill

Slussen has been used by people since 14th century so that there is man-made fill from different historical periods due to human activities. It contains wooden structures with high archaeological values (Stockholms Stad, 2017). Fillings were assumed to have same properties for each cross section, details are listed in Table 2.

Table 2 Properties of fill (Hardening soil, drained)

Parameter	Value
Unsaturated unit weight γ_{uns}	18 kN/m^3
Saturated unit weight γ_{sat}	20 kN/m^3
Cohesion c	0 kPa (5 kPa during $\varphi - c$ reduction)
Friction angle φ	32°
Dilatancy angle ψ	2°
Secant stiffness in standard drained triaxial test E_{50}^{ref}	20 MPa
Tangent stiffness for primary oedometer loading E_{oed}^{ref}	26.9 MPa
Unloading reloading stiffness E_{ur}^{ref}	80 MPa
Power m	0.6
Initial void ratio e_{ini}	0.8
Poisson's ratio υ	0.2
Permeability k_x k_y	1 m/s

Table 3 Properties of sand (MC-model, drained)

Parameter	Value
Unsaturated unit weight γ_{uns}	19 kN/m^3
Saturated unit weight γ_{sat}	19 kN/m^3
Cohesion c	0 kPa
Friction angle φ	35.6°
Dilatancy angle ψ	0°
Young's Modulus E	23.3 MPa
Poisson's ratio υ	0.2
Permeability k_x k_y	1 m/s

4.3.2.1. Sand

There is at least one sand layer under all the cross sections and they were assumed to have same properties as well, see Table 3.

4.3.2.2. Organic clay

Organic clay is considered to be undrained that could lead to soil failure due to construction. All the parameters were taken from results of CPT tests (Table 4). The undrained shear strength among all the cross sections was chosen as 50 kPa for the deterministic calculations. This value is much lower than the average value from CPT tests due to conservative concerns. But the mean value of Young's Modulus E from CPT tests was used.

Table 4 Properties of organic clay (MC-model, undrained B)

Parameter	Value
Unsaturated unit weight γ_{uns}	19 kN/m^3
Saturated unit weight γ_{sat}	19 kN/m^3
Undrained shear strength c_u	50 kPa
Young's Modulus E	18 MPa
Poisson's ratio υ	0.3
Permeability k_x k_y	10^{-9} m/s

Table 5 Properties of organic clay/mud (MC-model, undrained B)

Parameter	Value
Unsaturated unit weight γ_{uns}	19 kN/m^3
Saturated unit weight γ_{sat}	19 kN/m^3
Undrained shear strength c'_u	40 kPa
Young's Modulus E	18 MPa
Poisson's ratio υ	0.3
Permeability k_x k_y	10^{-9} m/s

4.3.2.1. Organic clay/mud

There are soft mud layers on the west side of Slope R1 as well. These mud layers are quite sensitive so that attentions needed to be drawn to them. c_u of this type of clay is assumed to be around 80% of the c_u of organic clay. As a result, properties are shown in Table 5.

4.3.2.2. Esker gravel

Granular layers exist from the Stockholm esker layer between clay layer and bed rock, which have no cohesion but high strength and friction angle. In this project it was also assumed that all granular soil layers are the same (Table 6).

Table 6 Properties of granular soil (MC-model, drained)

Parameter	Value
Unsaturated unit weight γ_{uns}	18 kN/m^3
Saturated unit weight γ_{sat}	20 kN/m^3
Cohesion c	0 kPa
Friction angle φ	33°
Dilatancy angle ψ	3°
Young's Modulus E	81.5 MPa
Poisson's ratio υ	0.3
Permeability k_x k_y	1 m/s

4.4. Design load and factor of safety

The design traffic load from metro is defined as a line load of 65 kN/m over a width of 2.25 m so that the characteristic value for traffic load is then the pressure 29 kPa (Storstockholms Lokaltrafik AB, 2009).

The characteristic design loads from different kinds of machinery on site are assumed to be 20 kPa. It is also assumed that this load is distributed all over the working surface until it is 9 m away from the site border. (Storstockholms Lokaltrafik AB, 2009).

The partial coefficient is determined to be 1.27 according to the safety classes (Karlsson, M. & Moritz, L., 2014). As a result, the final design loads are listed in Table 7.

Table 7 Design load for metro and machinery

Design Load	Characteristic values	Partial coefficient	Final Value
Metro(Traffic)	29	1.27	36.7
Machinery	20	1.27	25.4

Table 8 Limited value for factor of safety

Safety class	Analysis methods	
	Undrained	Drained or combined
1	1.35	1.20
2	1.50	1.30
3	1.65	1.40

In Sweden, the limit values of factor of safety in soil are defined by Trafikverket depending on the safety class and analytical methods (Karlsson, M. & Moritz, L., 2014). Table 7 can be applied regardless of design load type and material parameters. Safety class 3 is chosen for Slussen project so that a certain safety factor according to Table 8 should be reached depending on the drainage situation for all the cross sections in Slope R1.

4.5. Field monitoring

Various field monitoring systems are installed in Nya Slussen project to ensure the safety on site. Intensive monitoring is highly demanded by Slope R1 due to its safety class and location. Therefore, a monitoring system using inclinometers and 3D deformation sensors was developed for Slope R1.

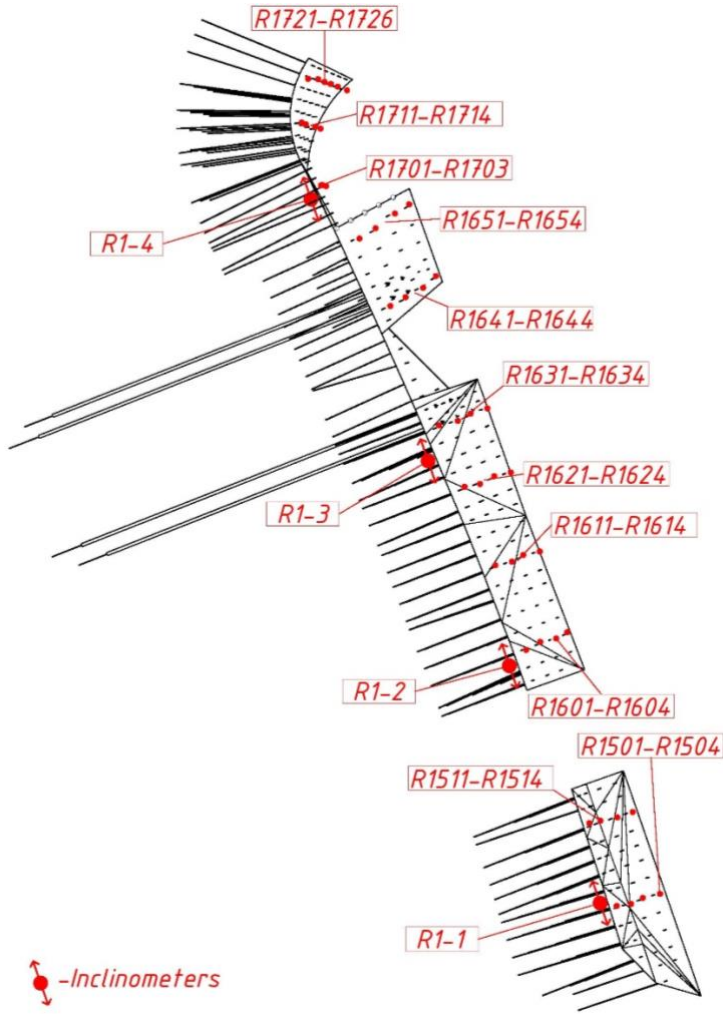

Figure 23: Location of inclinometers and 3D-measurement points

As shown in Figure 23, the monitoring system consists of 4 inclinometers (R1-1 to R1-4) and 45 3D-measuring points that are distributed all along Slope R1. Near CS1 there is one inclinometer and 8 3D-measuring point while CS2 and CS3 have two inclinometers with 16 3D-measuring points. Because the slope near CS4 is quite steep, it has one inclinometer with 21 3D-measuring points. All the measurements are performed at the same time as the excavation process and updated on the internet.

Figure 24 shows the current construction process and inclinometer system on site. All the 3D-measuring points and inclinometer data loggers on the wall are connected to the internet so that all the measured data can be updated in time. The inclinometer installed in this project is Slope inclinometer ITS series HD.

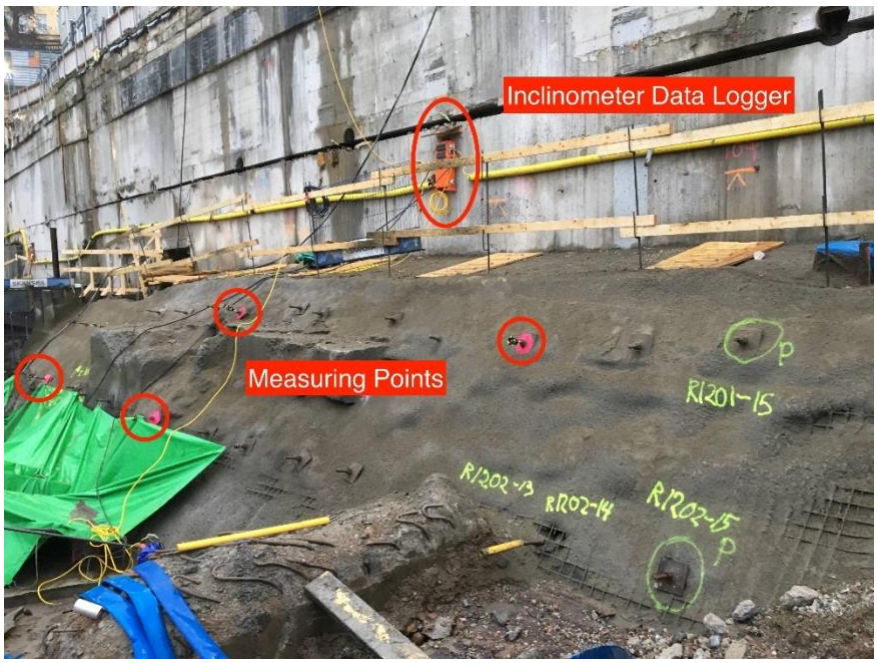

Figure 24: Field photo of the measurement system

4.6. Deterministic design

The construction process was analyzed by finite element program Plaxis 2D. All the geometry details, geological conditions and design load were modelled into Plaxis to study the stability of Slope R1. As one of the most used deterministic methods, FEM analysis can provide an estimation of the ground behaviors that correspond to construction.

4.6.1. Model setup

Four individual geometrical Plaxis models with different geometry and geological conditions were built for CS1 to CS4, respectively. Existing concrete foundation, ballast material, soil nails and shotcrete were also modelled into Plaxis with different properties. Their properties are shown in Table 9. Additionally, characteristic values for traffic load were used in this deterministic simulation.

Table 9 Properties of other structures

Name	Type	Model	Properties
Ballast	Soil	MC Drained	$\gamma_{uns} = 19\ kN/m^3$ $\gamma_{sat} = 21\ kN/m^3$ $E = 150\ MPa \quad \upsilon = 0.2$ $c = 0\ kPa\ \ \varphi = 40°\ \ \psi = 5°$ $k_x\ k_y = 1\ m/s$
Concrete		Linear Elastic Non-porous	$\gamma = 25\ kN/m^3$ $E = 30\ GPa \quad \upsilon = 0.2$
Soil nailing	Embedded beam row	Elastic Massive circular pile	$E = 30\ kN/m^2 \quad m = 0.05$ $L_{spacing} = 1.2m$ $T_{skin} = 20\ kN/m$
Shotcrete	Plate	Elastic	$EA = 2.5 \cdot 10^6\ kN/m$

			$EI = 2.083 \cdot 10^5\ kN \cdot m^2/m$ $\omega = 5\ kN/m/m \quad \upsilon = 0.2$

4.6.2. Stage construction

In Plaxis, stage construction is quite important because it controls the timing and order of construction activities. The stage construction of Nya Slussen was modelled as following:

- Initial phase: Gravity loading of the ballast, metro's foundation and traffic load.
- Phase 1: Reset displacement. Application of machinery load.
- Phase 2: Excavation until 0.5 m below the first soil nail and change of the level of machinery load.
- Phase 3: c - φ reduction safety analysis for the current situation.
- Phase 4: Installation of shotcrete and soil nail.
- Phase 5: Consolidation phase until next excavation phase.
- Phase 6-13: Repetition of Phase 2 to 4 until the excavation reaches the bottom.
- Phase 14-17: Consolidation phase until measuring data was taken.
- Phase 18: Total c - φ reduction safety analysis of the final situation with full depth excavation and full slope support, but without machinery load.

4.6.3. Result

Factor of safety of each construction phase in different cross sections were computed by Plaxis and the failure mechanism of Slope R1 was plotted into colorful figures. Their factors of safety are summarized in Table 10. All the factors of safety have reached the minimum requirement 1.65 for slide in the undrained soil layers, and 1.4 for slide in the drained soil layer.

Table 10 Summary of factor of safety and total displacement

Cross section	CS1	CS2	CS3	CS4
Drainage type	Undrained	Drained	Drained	Undrained
Required FS	1.65	1.40	1.40	1.65

Reached FS	1.67	1.80	1.54	1.70
Maximum total displacement/mm	36	41	59	54

4.6.3.1. CS1

From the result of CS1, the incremental strain figure shows almost the same failure boundaries as the total displacement figure. A semi-circular failure zone was indicated while incremental strains also concentrated at the foot of Slope R1 (Figure 25).

4.6.3.1. CS2

The situation of CS2 is slightly different from CS1. With the same c_u applied, the model showed a drained failure surface that excluded the clay layers (Figure 26). The maximum total displacement was then 41 mm and it happened deeper under the excavation. The failure zone in this case was much smaller than the one showed in Figure 25 and strains were concentrating on the foot of the slope. The factor of safety is 1.80, much larger than 1.4 in the requirement for drained conditions.

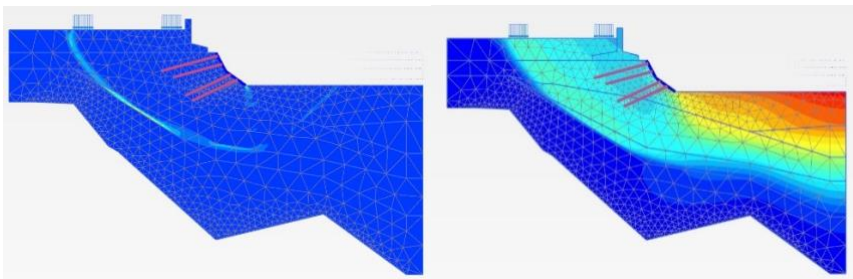

Figure 25: (a) Failure mechanism of CS1 (b) Total displacement of CS1

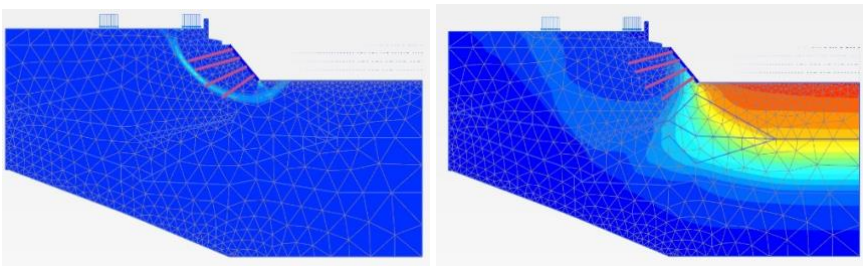

Figure 26: (a) Failure mechanism of CS2 (b) Total displacement of CS2

4.6.3.2. CS3

CS3 had a maximum displacement of 59 mm that is higher than CS1 and CS2. But most of the displacement occurred around the excavation, especially the bottom of it. CS3 showed drained failure surface hence the limitation for factor of safety is only 1.40. Perhaps it was influenced by the near-surface drained sand layer between filling and organic clay (Figure 27).

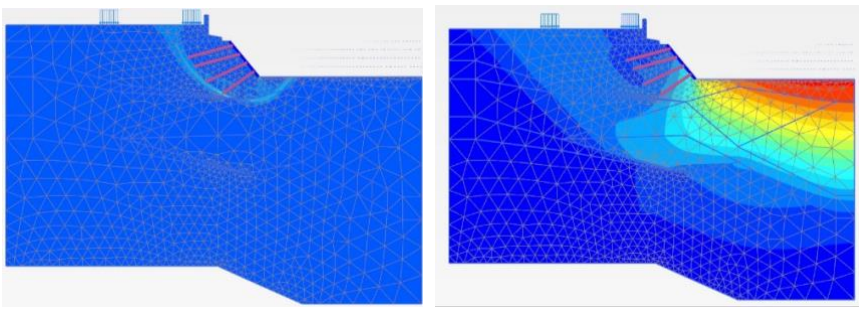

Figure 27: (a) Failure mechanism of CS3 (b) Total displacement of CS3

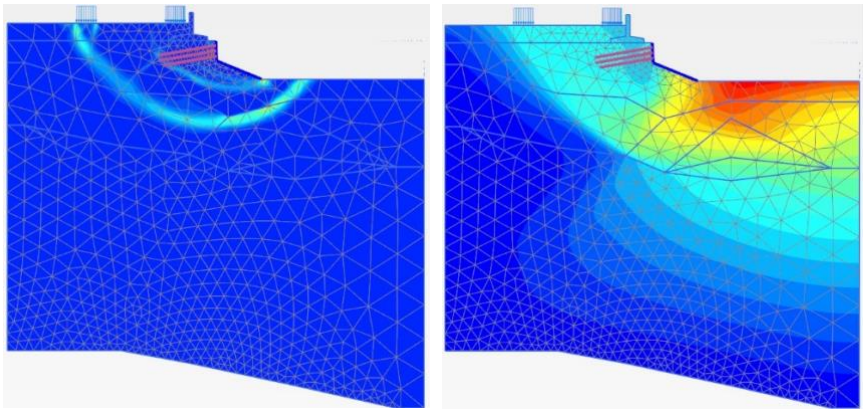

Figure 28: (a) Failure mechanism of CS4(b) Total displacement of CS4

4.6.3.1. CS4

CS4 had a circular failure surface under the slope with a maximum displacement of 54 mm. The failure surface showed perfect boundaries that it connected the foot of Slope R1 and existing metro ballast. Displacement occurred around the excavation thus CS1, CS2 and CS3 had the similar distributions while CS4 had different distribution. A factor of safety of 1.70 was reached (Figure 28).

4.7. Uncertainties and comments

As described in the previous chapters, there are plenty of uncertainties existing in many aspects of geotechnical engineering because sometimes soil can be very complicated to study. For example, it is difficult to determine the boundaries between different soil layers even though a large amount of investigations have been performed. The geotechnical conditions between two boreholes will always contain uncertainties.

The uncertainties remaining within the deterministic methods cannot be neglected if a more reliable result is expected. Focus should be drawn on the uncertainties within soil parameters specifically. There are several empirical assumptions made for soil parameters within Plaxis simulation. Among those assumptions, undrained shear strength and Young's modulus of different soil layers take up most of the uncertainties. Therefore, further studies regarding the uncertainties within soil parameters has been carried out in the next chapter.

5. Case study: application of the methodology in the Slussen project

In the previous chapter, the finite element method (FEM) was applied as a deterministic tool to assess the stability of Slope R1. But there are still uncertainties associated with it. In the current chapter, the stability of slope R1 has been assessed by means of the methodology developed in chapter 3. Several probabilistic tools mentioned before will be tested like point estimation and event tree.

5.1. Uncertainties remaining in the deterministic method

As mentioned in Chapter 2, uncertainties exist in most of the deterministic methods, especially within the soil parameter determinations. There are many assumptions and simplifications made for the Plaxis calculations. c_u of organic clay was chosen as 50 kPa regardless of the measured data from Cone Penetration Test (CPT). As a result, it is better to apply the approach developed in chapter 3 to assess slope stability of Slope R1 since probabilistic methods take variations of soil parameters into account.

5.2. Flowchart of the case study

A general flowchart has been presented in the previous chapter with descriptions of each section. In this chapter it is specified for evaluation of the stability of Slope R1 in Nya Slussen project (Figure 29).

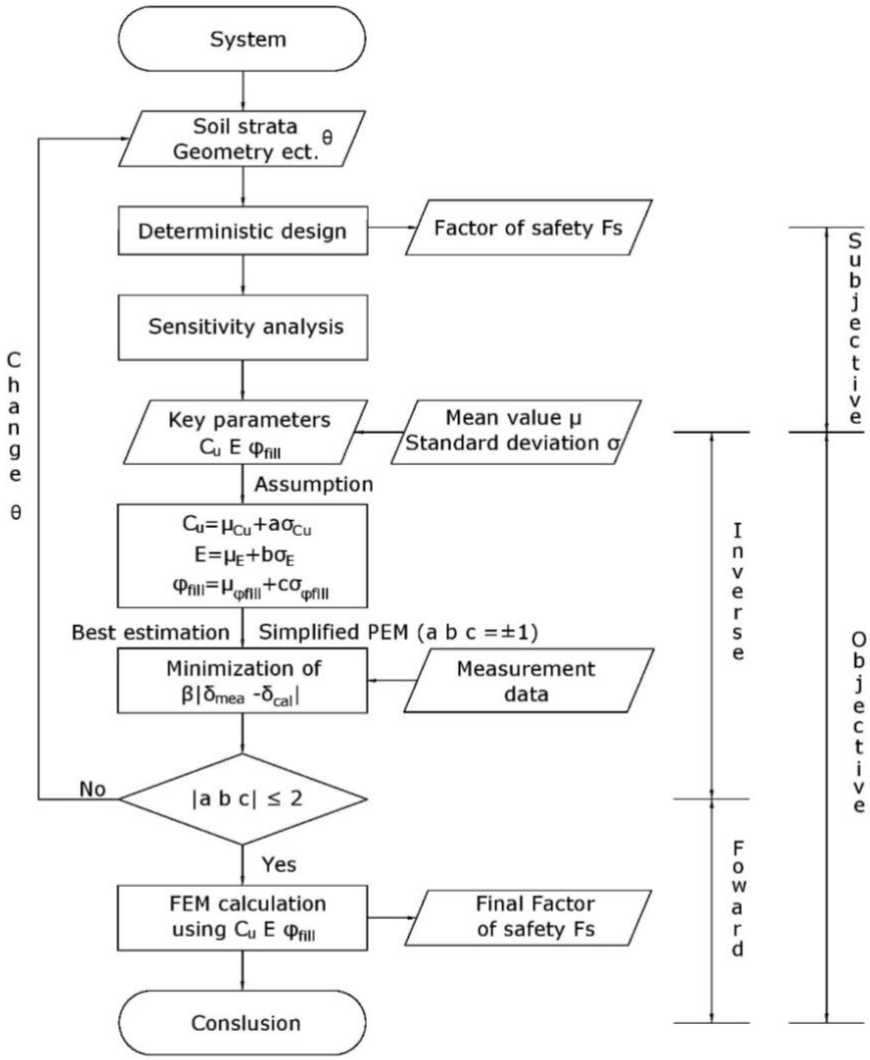

Figure 29: Flowchart of the case studies

5.3. Measurement data

As mentioned in the last chapter, there are two different measurement systems that have been used in Nya Slussen project. Inclinometers focus on the horizontal displacement occurring along a certain depth under

Slope R1 while 3D-measuring points monitor the three-dimensional deformation of the surface of Slope R1. In this project, all measuring data were obtained from 2017.10.06 to 2018.04.05. Note that some inclinometers and 3D-measuring points were installed during this period with construction phases so that their measuring data only started from the day they were installed. CS1 was chosen to be performed the methodology because it has the closest factor of safety to its limit, hence it is more typical and interesting.

5.3.1. Inclinometer

The inclinometer has a series of measuring points with an interval of 1 m following the depth under Slope R1. In order to visualize how deformation develops with construction phases, measuring data was taken following the excavation process and every month after final excavation.

Inclinometer R1-1 was installed on 2017.10.06. and it has 14 measuring elevation between 4 m and -9 m with 1 m interval (Figure 30). Horizontal displacement developed within the excavation process with a few days of time delay. Such displacement still increases above the excavation level after the final excavation while it stopped increasing in the subsoil.

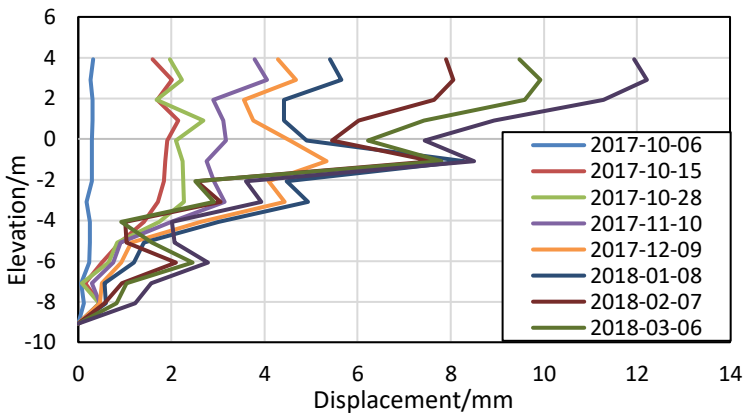

Figure 30: Horizontal displacement of CS1 (R1-1)

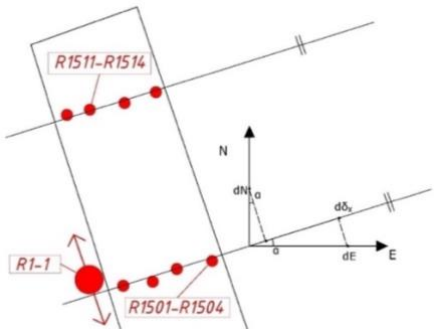

Figure 31: Direction of 3D-measurement

5.3.2. 3D-measurement

In the 3D-measuring system, only displacements following North-East directions (dN, dE) and vertical direction (dH) are recorded so that it is important to convert those raw data to the axis that is perpendicular to Slope R1 (Figure 31). Assume that the angel between East direction and slope's perpendicular line is α, the total displacement can be calculated as Equation 5.1 and 5.2. The displacement following the direction of Slope R1 is neglected due to its unimportance.

$$d\delta_x = dN \cdot sin\,\alpha + dE \cdot cos\,\alpha \quad (5.1)$$

$$d\delta_y = dH \quad (5.2)$$

Where δ_x is the horizontal displacement and δ_y is the vertical displacement. All the measuring point are located on the surface of Slope R1 and they are installed gradually following the construction process. For CS1, CS2 and CS3, measuring data collected every hour are here obtained every half month in order to show the development of deformations of Slope R1. Since measuring points near CS4 were installed on 15.03.2018, their data was taken every five days.

There are two series of 3D-measuring points near CS1 (R1501-R1504, R1511-R1514). The total displacement components are calculated as the average between those two series and this rule is also applied to other cross sections. For example, the settlement at first soil nail was taken from the

mean value between R1501 and R1511. The earliest measuring data were recorded on 10/11/2017.

Figure 32 indicate the gradual growth of both horizontal and vertical displacement near CS1. However, the purple line (R1504 and R1514) showed unregularly development of both settlement components. Their vertical displacement is much larger than other measuring points. A simple explanation is that the measuring points were disturbed by local construction procedure that leads to unreasonable data distribution.

3D-measuring are not performed throughout the whole excavation procedure, focus was hence more concentrated on inclinometers.

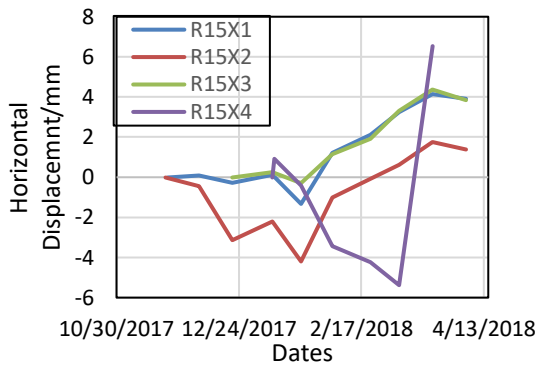

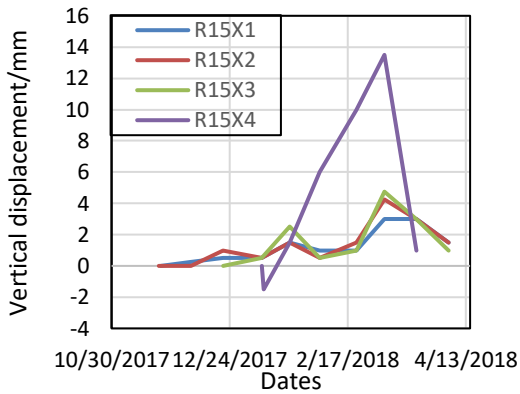

Figure 32: Total displacement of CS1

5.3.3. Summary of the displacement measurements

To summarize all the measuring data in a systematic way with respect to the construction's schedule, a new table was created (Table 11).

Table 11 Summary of measurement data of CS1

Date / Point	2017-10-06	2017-10-15	2017-10-28	2017-11-10	2017-12-09	2018-01-08	2018-02-07	2018-03-06	2018-04-05
Horizontal displacement in the soil Δ_x/mm									
4	0.32	1.60	1.97	3.79	4.29	5.40	7.90	9.48	11.95
3	0.27	2.02	2.23	4.05	4.67	5.65	8.06	9.93	12.21
2	0.31	1.70	1.68	2.89	3.55	4.41	7.64	9.59	11.28
1	0.31	2.15	2.69	3.12	3.76	4.42	6.02	7.43	8.93
0	0.29	1.91	2.10	3.17	4.55	4.91	5.44	6.23	7.44
-1	0.29	1.86	2.24	2.76	5.33	8.29	7.61	7.80	8.51
-2	0.29	1.84	2.26	2.91	4.09	4.48	2.55	2.51	3.61
-3	0.18	1.71	2.27	3.15	4.44	4.93	3.06	2.91	3.93
-4	0.25	1.41	1.73	2.00	2.62	3.02	1.00	0.92	2.02
-5	0.25	0.89	0.83	0.92	1.14	1.40	1.03	1.58	2.07
-6	0.23	0.51	0.65	0.74	0.92	1.19	2.10	2.46	2.78
-7	0.06	0.15	0.08	0.29	0.51	0.56	0.94	1.04	1.56
-8	0.12	0.46	0.46	0.46	0.46	0.60	0.57	0.82	1.22
-9	0.00	0.00	0.00	0.00	0.00	0.00	0.00	0.00	0.00
Horizontal displacement on the slope δ_x/mm									
R15X1	-	-	-	0	0.58	0.11	0.92	1.61	3.92
R15X2	-	-	-	0	1.25	-2.28	-1	0.62	1.38
R15X3	-	-	-	-	-	0	1.14	3.31	3.85
R15X4	-	-	-	-	-	0.92	-2.91	-5.38	-
Vertical displacement on the slope δ_y/mm									
R15X1	-	-	-	0	1	0.5	0.5	1.5	1.5
R15X2	-	-	-	0	0	0.5	1.5	4.25	1.5

R15X3	-	-	-	-	-	1	1.5	4.75	1
R15X4	-	-	-	-	-	-1.5	6.5	13.5	-

5.4. Systematic analysis

In this part, previous FEM modelling results were compared with the measuring data after some key parameters are determined by a sensitivity analysis. Then inverse analysis was conducted to find the suggested values for those parameters. At the end a total safety factor was calculated through forward calculation using those suggested parameters. Due to the lack of time and resources, systematic analysis was only performed on CS1 since it is the most representative cross section of Slope R1 and has the closest factor of safety to its limit, which makes it more interesting to study.

5.4.1. Sensitivity analysis

The application of a sensitivity analysis was simplified in Slussen project. In this case, input data is the variation of soil parameters underground while the FEM models used in the last chapter are the subjects. An empirical range is made for each parameter. Each Plaxis model was run dozens of times with respect to the variety of different parameters. When a certain parameter was tested, other parameters stay at the same value as the deterministic design. It only allowed one variable in each analysis. Generally, the most uncertainties are concentrated in undrained clay layers so that c_u, E and K_0 were selected for sensitivity analysis. The assumption that its c_u equals 80% of organic clay is still applied here because of the lack of knowledge about organic clay/mud. Meanwhile, the same parameters were analyzed for fill as well as its φ_{fill}. Sometimes φ_{fill} can be very critical in reality, so it was tested in the models along with E for sand and gravel. The criterion is the total safety factor and maximum displacement that obtained from Plaxis 2D.

After a series of testing and modelling, it was found that the c_u and E of both undrained organic clay layers had significant influence on the total stability. Nevertheless, the φ_{fill} was subsequently determined as the third

parameter that affects the safety factor. Other parameters showed neglectable impacts on the total stability or deformation of Plaxis model hence they are not specifically presented here.

Undrained shear strength c_u was tested at the range between 10 kPa for organic clay; 8 kPa for organic clay with mud to 70 kPa for organic clay; 56 kPa for organic clay with mud. The results indicated that c_u had the major impact on the total stability. The model showed soil failure when c_u was less than 25 kPa for organic clay; 20 kPa for organic clay with mud. Both deformation and factor of safety had great variation when different values of c_u were tested. There is no doubt that c_u is the most important factor of total stability (Figure 33(a)).

Young's Modulus E was tried between 10 MPa to 26 MPa for both types of organic clays. As a result, the factor of safety stayed around the same level as deterministic design while the maximum displacement varied rapidly when lower values of E were applied (Figure 33(b)).

The friction angle of fill φ_{fill} was selected from 28° to 38° as the normal range of φ_{fill} in nature. As the two parameters above, the factor of safety and deformation changed slightly corresponding with φ_{fill} (Figure 33(c)).

These three parameters were hence selected, and they would be analyzed systematically in the objective studies in the following steps.

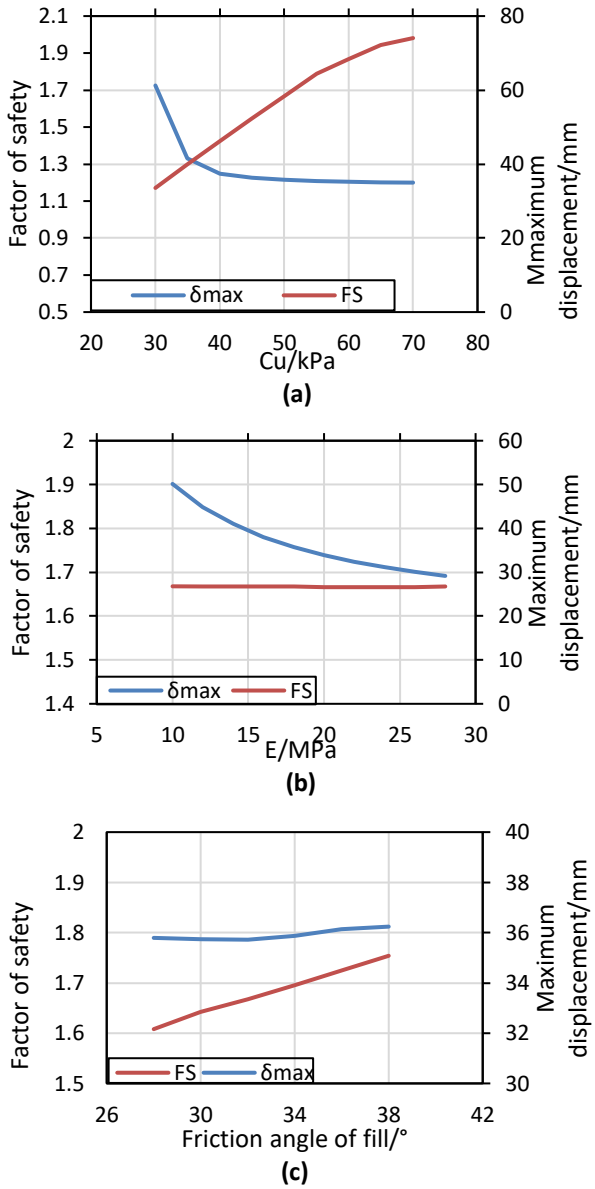

Figure 33: Key parameters determined from sensitivity analysis

5.4.2. Parameters from CPT testing

Since the key parameter have already been chosen, it is vital to figure out their distribution in a probabilistic way. In the deterministic design, all the parameters were selected according to different empirical assumption or approximation. In this chapter, all the raw data from CPT in-situ tests were analyzed throughout probabilistic tools. The first step is to assign a distribution form to those key parameters.

There is a CPT-testing borehole near each cross section. Since all the cross sections have same types of soil but with different soil distributions, raw data from all the boreholes (14E051, 16E001, 16E002 and 16E003) was summarized and proceeded together.

In deterministic design, a c_u of 50 kPa was used for organic clay while 40 kPa was used for organic clay/mud. However, they were both assumed and conservative values aiming to fulfill the requirement of factor of safety that are much lower than the reality from CPT tests. From CPT tests, the mean value of c_u is 176. kPa with a standard deviation of 80 kPa. Lognormal distribution was then applied due to the high value of standard deviation. The purpose is to nominate the negative values in the normal distribution since they do not exist in nature. Figure 40 showed both types of distribution for better illustration (Figure 34(a)).

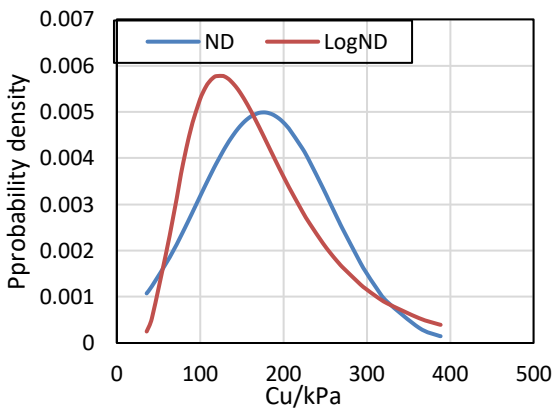

(a)

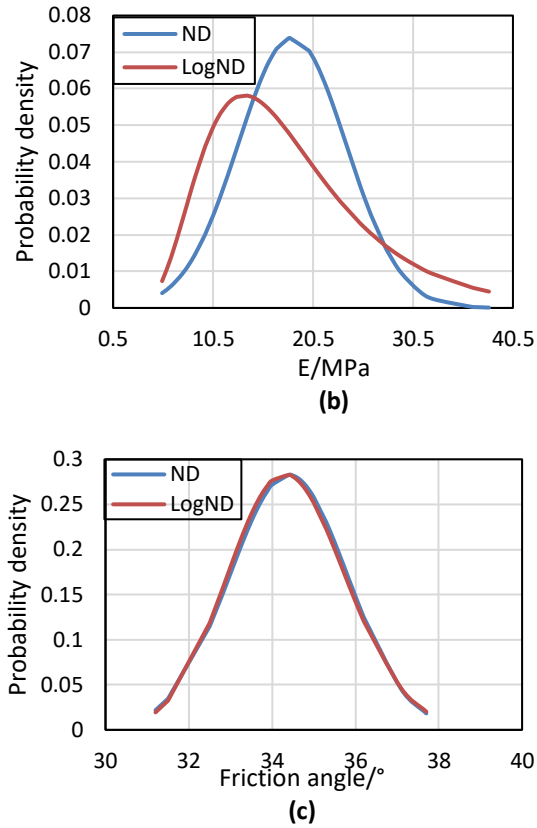

Figure 34: Probability distribution of the key parameters

Young' modulus for both types of clay was selected at its mean value from CPT tests (18 MPa). The standard deviation is 5.4 MPa. For the purpose of avoiding negative values, lognormal distribution was also chosen for E (Figure 34(b)).

The friction angle of fill was set as 32° in deterministic design due to conservative concern. From CPT tests, its mean value is 34.4° while its standard deviation is 1.4°. Both normal distribution and lognormal distribution provided similar results. The normal distribution was hence used in order to simplify the calculation process (Figure 34(c)).

However, the various distributions only help to give a better illustration of key parameters since only mean values and standard deviations were taken from them. The forms of data distribution do not play any important roles for the inverse analysis. As a result, the limit factor γ for inverse analysis was chosen as 2 since there is very low possibility that the target value will drop out of the range $\mu \pm 2 \cdot \sigma$.

5.4.3. Inverse analysis

In this step, three key parameters from sensitivity analysis were modelled into Plaxis 2D with their probabilistic values from CPT tests. Following the methodology developed in Chapter 3, three different factors ($a\ b\ c$) were assigned to them together with their mean values μ and standard deviations σ. Hence the parameters are expressed in Equation (5.3-5.5).

$$c_u = \mu_{c_u} + a \cdot \sigma_{c_u} = 176.4 + a \cdot 80 \tag{5.3}$$

$$E = \mu_E + b \cdot \sigma_E = 18 + b \cdot 5.4 \tag{5.4}$$

$$\varphi_{fill} = \mu_{\varphi_{fill}} + c \cdot \sigma_{\varphi_{fill}} = 34.4 + c \cdot 1.4 \tag{5.5}$$

The methodology includes finding proper values of $a\ b$ and c so that the difference of displacement between the modelled and the measured can be minimized according to Equation 3.2. A corresponding weight factor β_i was given to every elevation of inclinometer measurement. Values of weight factors were chosen manually depending on the subjective quality of measurement. The best approach is to use Monte Carlo Method by repeating the simulation with random values of $a\ b$ and c, but it consumes too much time. Therefore, a simplified optimization method inspired by Point Estimation Method was then proposed for this case.

5.4.3.1. Simplified point estimate method

As mentioned in Chapter 2, 8-point estimation is suitable if there are three different variables to be estimated (Equation 2.19-2.22 and Figure 5). Additionally, the center point with only mean values from all the parameters was considered to reach a better estimation so that it becomes

a 9-point Point Estimation. However, weight factors ρ of Point Estimation were neglected since it has been considered in the main equation. As a result, all the 9 points were listed in Table 12.

Table 12 Point estimation of 9 points

Point	a	b	c	c_u /kPa		E /Mpa	φ_{fill} /°
				Org clay	Clay/mud		
1	0	0	0	176.4	141.1	18	34.4
2	1	1	1	256.4	205.1	23.4	35.8
3	-1	1	1	96.4	77.1	23.4	35.8
4	1	-1	1	256.4	205.1	12.6	35.8
5	1	1	-1	256.4	205.1	23.4	33
6	1	-1	-1	256.4	205.1	12.6	33
7	-1	1	-1	96.4	77.1	23.4	33
8	-1	-1	1	96.4	77.1	12.6	35.8
9	-1	-1	-1	96.4	77.1	12.6	33

Table 13 Weight factor corresponding to each elevation

β_i	Elevation
0.2	4
0.3	3
0.4	2
0.5	1
0.6	0
0.5	-1
1	-2
1	-3
0.6	-4
0.6	-5
0.5	-6
0.4	-7
0.7	-8
0.5	-9

All the 9 points were tested through previous Plaxis model to compute the deformations of inclinometer R1-1 under Slope R1. However, it showed big difference between the measurement and the simulation near ground surface level. As a result, weight factors β_i were applied to each elevation level with especially low values near surface and high values where the difference is smaller (Table 13).

The results for each point are attached in the Appendix. Results varied with different combinations of factors *a b* and *c* (Figure 35). Among them point 7 showed least total difference between measurement and simulations (126.7 mm) along with a medium factor of safety (2.22). The result did not show serious difference of factors of safety, but it varied much for total difference of displacement.

The result from the best fit point helped to locate the aiming values of *a b* and *c* by giving rough ranges of them. Then the optimization phase can hence be performed to find the best combination of *a b* and *c* by testing different values based on the result from the best point.

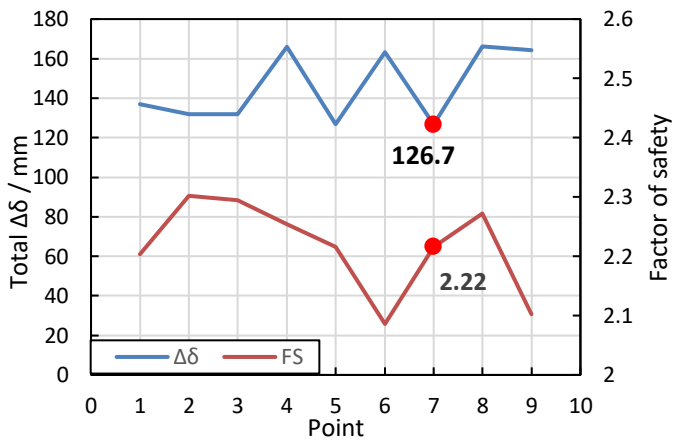

Figure 35: $\Delta\delta_{total}$ from 9-point estimation

5.4.3.2. Optimization of three parameters

The best fit point from point estimation provided a rough combination of a b and c where $a = -1$, $b = 1$ and $c = -1$. The optimization produce was carried out base on that range. Due to the potential correlation between c_u and E of organic clay, φ_{fill} of fill was tested and optimized first.

In previous deterministic design, φ_{fill} of fill was selected to be 32° as empirical value. When testing different values of c for the φ_{fill}, the other two parameters stayed the same as the best combination of point estimation (c_u=96.4 kPa/77.12 kPa, E=23.4 MPa). The testing range of c was between 0 and -2 since $c = -1$ gave the best estimation, which corresponds to the range from 34.4° to 31.6° for fill's friction angle. 10 different combinations were tested resulting in different $\Delta\delta_{total}$ factors of safety (Table 14).

Table 14 Optimization of friction angle of fill

Combination	a	b	c	φ_{fill}/°	$\Delta\delta_{total}$/mm	FS
10	-1	1	-2	31.60	125.1	2.04
11	-1	1	-1.7	32.02	126.2	2.06
12	-1	1	-1.5	32.30	127,0	2.09
13	-1	1	-1.4	32.44	127.3	2.09
14	-1	1	-1.3	32.58	125.8	2.09
15	-1	1	-1.2	32.72	126.1	2.11
16	-1	1	-1.1	32.86	126.4	2.22
17	-1	1	-0.8	33.28	126.9	2.14
18	-1	1	-0.6	33.56	128.6	2.16
19	-1	1	-0.2	34.12	130.5	2.20
20	-1	1	0	34.40	130.7	2.22

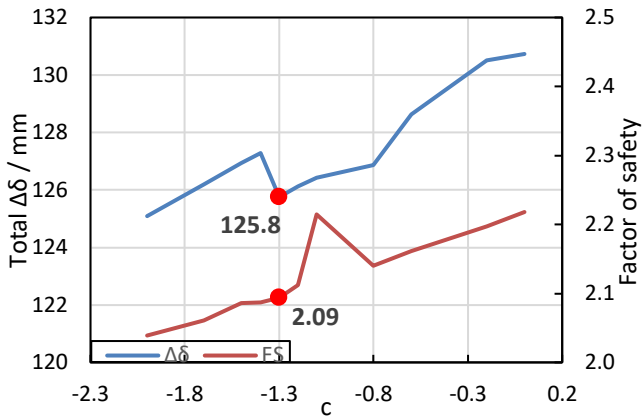

Figure 36: $\Delta\delta_{total}$ and FS from c value estimation

It turned out that the lowest value of $\Delta\delta_{total}$ occurred when $c = -2$ and $\varphi_{fill} = 31.60°$. However, it does not fulfill the requirement of the limit factor γ=2. Therefore, the optimized value of c and φ_{fill} is chosen as $c = -1.3$ and $\varphi_{fill} = 32.58°$. Also, it stayed at the same values while the other two parameters are examined (Figure 36).

The second parameter to be studied is E of clay. Since it is a sensitive parameter that influences the deformation of soil, 15 combinations were tested to find a minimum difference between the measurement and the calculations (Table 15).

The $\Delta\delta_{total}$ decreased with the increase of b and E until it reached the minimum point where $b = 1.8$ and $E = 27.72\ MPa$. Although it did not show much difference from the optimization of c, the minimum point still could be considered as a successful optimization. But due to the potential correlation between c_u and E of organic clay, further check was needed to be made to ensure the accuracy of this optimization (Figure 37).

Table 15 Optimization of Young's Modulus of organic clay

Combination	a	b	c	E/MPa	$\Delta\delta_{total}$/mm	FS
21	-1	2	-1.3	28.80	126.4	2.10
22	-1	1.9	-1.3	27.72	125.6	2.11
23	-1	1.8	-1.3	26.64	125.4	2.10
24	-1	1.7	-1.3	25.56	127.5	2.10
25	-1	1.6	-1.3	24.48	127.4	2.10
26	-1	1.5	-1.3	22.32	125.6	2.10
27	-1	1.4	-1.3	21.24	125.5	2.10
28	-1	1.3	-1.3	20.16	125.5	2.10
29	-1	1.2	-1.3	19.08	125.6	2.09
30	-1	1.1	-1.3	18.00	125.7	2.11
31	-1	0.8	-1.3	28.26	127.3	2.09
32	-1	0.6	-1.3	27.18	128.0	2.09
33	-1	0.4	-1.3	26.10	129.4	2.08
34	-1	0.2	-1.3	25.02	130.7	2.09
35	-1	0	-1.3	23.94	133.7	2.11

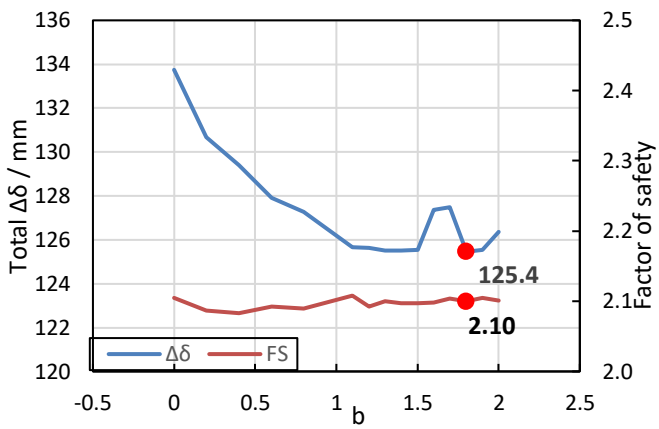

Figure 37: $\Delta\boldsymbol{\delta}_{\boldsymbol{total}}$ and FS from b value estimation

The undrained shear strength c_u of both types organic clays was tested by 13 different combinations (Table 16). The lowest value of a was -1.6 because any other values lower than -1.6 would cause failure in the Plaxis 2D model.

Table 16 Optimization of undrained shear strength of organic clay

Combination	a	b	c	c_u/kPa		$\Delta\delta_{total}$/mm	FS
				Org clay	Clay/mud		
36	-1.6	1.8	-1.3	48.4	38.72	220.3	1.64
37	-1.4	1.8	-1.3	64.4	51.52	131.3	1.95
38	-1.2	1.8	-1.3	80.4	64.32	127.2	2.07
39	-0.9	1.8	-1.3	104.4	83.52	125.5	2.10
40	-0.8	1.8	-1.3	112.4	89.92	125.4	2.11
41	-0.7	1.8	-1.3	120.4	96.32	125.5	2.10
42	-0.6	1.8	-1.3	128.4	102.72	125.4	2.10
43	-0.5	1.8	-1.3	136.4	109.12	125.4	2.11
44	-0.4	1.8	-1.3	144.4	115.52	125.5	2.12
45	-0.2	1.8	-1.3	160.4	128.32	125.5	2.12
46	0	1.8	-1.3	176.4	141.12	125.5	2.12
47	0.2	1.8	-1.3	192.4	153.92	125.5	2.12
48	0.4	1.8	-1.3	208.4	166.72	125.5	2.12
49	0.6	1.8	-1.3	224.4	179.52	125.5	2.12

The result showed little difference among all the combinations with $a > -1.2$ where Both $\Delta\delta_{total}$ and factors of safety fluctuated at a steady level. The lowest value of $\Delta\delta_{total}$ occurred when $a = -0.5$, which also provided a reasonable factor of safety (Figure 38).

So far, all the factors were optimized to their best values that correspond to the measurement. But the potential correlation between c_u and E of organic clay still needs to be considered and examined. Hence an extra optimization step was performed for E. c_u remained as the found value when $a = -0.5$ while b was tested for 9 different combinations to check if 1.8 was the best fit value (Table 17).

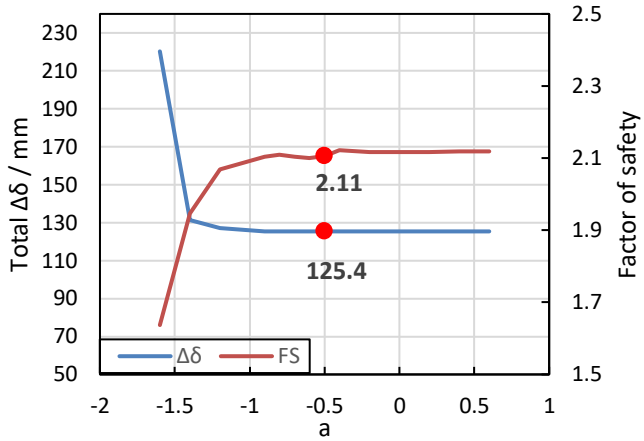

Figure 38: $\Delta\boldsymbol{\delta}_{\boldsymbol{total}}$ and FS from a value estimation

Table 17 Second optimization of Young's Modulus of organic clay

Combination	a	b	c	E/MPa	$\Delta\delta_{total}$/mm	FS
50	-0.5	1.9	-1.3	28.26	128.0	2.11
51	-0.5	1.8	-1.3	27.72	125.4	2.11
52	-0.5	1.7	-1.3	27.18	127.4	2.11
53	-0.5	1.6	-1.3	26.64	127.4	2.11
54	-0.5	1.5	-1.3	26.1	125.5	2.11
55	-0.5	1.4	-1.3	25.56	125.5	2.10
56	-0.5	1.3	-1.3	25.02	125.5	2.11
57	-0.5	1.2	-1.3	24.48	125.6	2.10
58	-0.5	1.1	-1.3	23.94	125.7	2.11
59	-0.5	1	-1.3	23.4	125.8	2.11

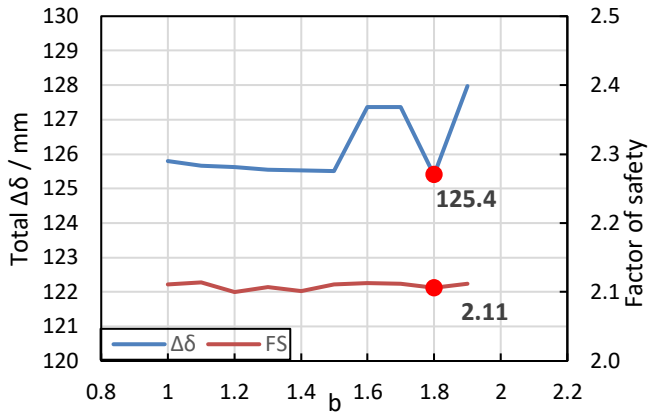

Figure 39: $\Delta\boldsymbol{\delta_{total}}$ and FS from b value second estimation

The lowest $\Delta\delta_{total}$ still occurred when $b = 1.8$, but with tiny difference among other values of b. The potential correlation was then reduced by this step because the best optimization has been found for all the parameters (Figure 39).

To conclude, simulation results of horizontal displacement from Plaxis 2D are optimized until the $\Delta\delta_{total}$ is minimized with respect to the field measurement when $a = -0.5, b = 1.8$ and $c = -1.3$. This optimized combination of factors was then proceeded into forward calculation for a final assessment of slope stability.

5.4.4. Forward calculation

In this step, all the parameters determined from inverse analysis were directly modelled into the Plaxis model to compute the final result. ($c_u = 136.4\ kPa$ for organic clay, $c_u = 109.2\ kPa$ for organic clay/mud, $E = 27.7\ MPa$ for both types of clay and $\varphi_{fill} = 32.6°$ for fill).

After simulation, the maximum total displacement of soil was 28.79 mm that mostly concentrated on the right boundary of the model (Figure 40(a)).

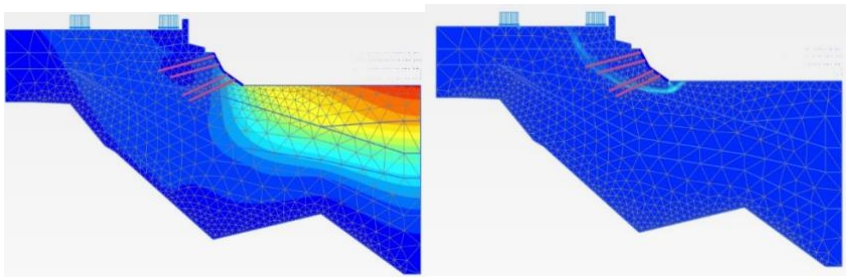

Figure 40: (a) Total displacement of CS1 (b) Failure mechanism of CS1

Table 18 Summary of horizontal displacement at the location of the inclinometer

Phases							
Excavation phases				Consolidation phases			
4	7	10	13	14	15	16	17
Horizontal placement distribution							
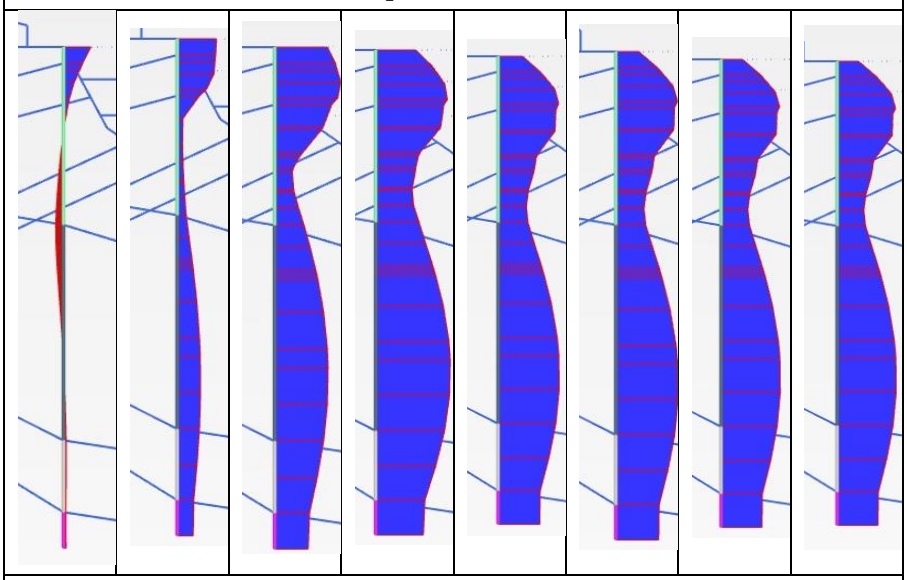							
Maximum horizontal placement/mm							
1.51	2.20	3.6	4.29	3.64	3.54	3.53	3.52

However, the failure mechanism indicated by incremental strain only occurred in the fill layer. The final safety factor was calculated as 2.106 with drained failure in the soil, probably because the final c_u was much higher than the value used in deterministic design (Figure 25). So, the failure mechanism does not reach the organic clay layer, leading to a lower requirement of factor of safety 1.45 (Figure 46(b)).

When a cross section representing the inclinometer was taken in to consideration, it showed the maximum horizontal displacement at the elevation +3.5 mm after all excavation activities have been carried out (Table 18). After that the total displacement kept decreasing until it reached the last day of measurement data due to consolidation.

6. Discussion and conclusion

The project has been completed and an iteration on the slope stability assessment methodology was developed successfully. Deterministic design and probabilistic design were carried out for Slope R1 in Nya Slussen project and they both reached reasonable results. In this chapter the two methods are discussed and some suggestions are given.

6.1. Discussion

Overall, the methodology has been utilized according to the original plan. However, there are still some assumptions and approximations carried out to simplify the procedure. Limitations also exist due to different reasons.

6.1.1. Limitation of 2D modelling

Since the finite element program used in this project is Plaxis 2D, it could be one of the biggest limitations, which might result in the divergence between the modelling and the measurements. In the Nya Slussen project, all the four cross sections were basically excavated under the same period so that the influences of nearby construction could be significant. However, impacts from excavation of other cross sections were neglected in Plaxis 2D.

For example, in Plaxis 2D, horizontal displacement at the location of inclinometer only increased until the last excavation phase, then it started to decrease following the consolidation phases. But in reality, the higher levels of inclinometer showed increasing horizontal displacement throughout the whole monitoring period, which was under the influence of nearby construction activities. Similar difference also occurred to the 3D-

measurement points where they did not show any changing pattern in reality. Therefore, only result from inclinometer was chosen for the analyses.

6.1.2. Numbers of key parameters

The number of variables determines the amount of work. In Rosenbluth's point estimate method, 2^n points need to be estimated when there are n variables. The amount of calculation will increase exponentially with the number of variables. Since a simplified point estimate was used in this project, similar limitation is also expected. There were only three key parameters chosen in this project, leading to 9 points to be estimated. But it could be quite time consuming when there are more than 3 parameters to be examined.

6.1.3. Subjective determination of factors a, b and c

The determination of factors a, b and c was quite subjective, because all the testing values of them were chosen manually at an interval of 0.1 or 0.2. The accuracy of the optimization phase only reached tenths where there are still uncertainties remaining. Although simplified point estimate method gave a rough estimation of target values, it still would be better if they can be found in a more objective way such as Monte Carlo method. Moreover, the correlations among different parameters are difficult to estimate as well. Even though an extra back check has been done in this project for E and c_u, it did not eliminate the effects of correlation between them. It requires much more simulations and iterations to reduce the effects of correlations. If there are more parameters to be examined with potential possibilities of correlations among them, a more effective approach should be proposed.

6.1.4. Choice of cross section and time consumption

In the case study, only CS1 was chosen to carry out probabilistic design since it has the closest factor of safety to its limit, which made it more interesting to be analyzed. The other reason is that probabilistic methods

consume much more time than deterministic methods. It would be more objective if the methodology is carried out for all the four cross sections.

6.2. Conclusion

6.2.1. Deterministic methods

In deterministic design, most of the soil parameters were used with their empirical values due to conservative concerns. The final factors of safety for all cross sections successfully met the minimum requirements. Specifically, CS1 had the closest factor of safety to its limit so that it was considered to be the critical cross section.

Deterministic methods are still the most common and straightaway approaches to assess slope stability in the industry. Since the empirical values are usually chosen for soil parameters, uncertainties still remain within the design process. Deterministic methods do not require complex connections with field measurement, because everything can be done before the actual construction phases.

6.2.2. Probabilistic methods

The results of the probabilistic analyses were reasonable, both back analyses and forward calculations reached expected results. The final factor of safety for CS1 was determined to be 2.1 that is much higher than the value from the deterministic analysis (1.7). The reason is that conservative soil parameter values were used in deterministic design. However, the final value of b (1.8) was very close to the manually set limit factor $\gamma = 2$. The resulting value of E of clay was then 27.72 MPa, which is quite high for clay. According to the methodology, iteration of changing input data should be done. But due to possible disturbance of construction activities of nearby cross sections, it is acceptable that such error exists, unless it exceeds γ.

6.2.3. Combination of both methods

It is proposed that both the deterministic design methods and the probabilistic design methods are utilized in future projects, depending on the construction stages.

Deterministic methods require only geometry and soil parameters from pre-construction investigations- They are suitable to be performed before the construction phase as preliminary design. It provided a general estimation about the consequence of construction activities.

After the construction has begun, it is better to switch to probabilistic methods since they can be coupled with field measurements. This allows the slope to be assessed in a systematical way instead of simply compare the measurement and deterministic values. When new measurement data is obtained, the analyses can be updated into the origin model by probabilistic methods. Hence the geometry or soil parameters can be calibrated with respect to the measurement, which makes them closer to the reality.

6.3. Future scope

As mentioned in the discussion, it is highly suggested that Monte Carlo method and 3D finite element program like Plaxis 3D are utilized in the methodology as a probabilistic tool to find the optimized values of soil parameters. Monte Carlo method functions by repeating random input values within a certain range for many times, which is suitable for this methodology. But there are still some questions to be solved.

Monte Carlo method is well known for its better estimation, but also the drawback of time consuming. Therefore, the methodology can only be used when there is no time limitation to obtain reasonable results. It is also difficult to connect Plaxis models to Matlab since each simulation is already a complicated finite element computation. This hence requires much work in programming. If these problems can be overcome, the slope

assessment methodology could be a very strong tool for the geotechnical industry.

7. References

Huang, R. and Li, W.L., 2008. Research on development and distribution rules of geohazards induced by Wenchuan earthquake on 12th May, 2008. Chinese Journal of Rock Mechanics and Engineering, 27(12), pp.2585-2592.

Abramson, L.W., 2002. Slope stability and stabilization methods. John Wiley & Sons.

Fredlund, D.G. and Krahn, J., 1977. Comparison of slope stability methods of analysis. Canadian Geotechnical Journal, 14(3), pp.429-439.

Barends, F.B., 2011. Introduction to soft soil geotechnique: content, context and application. Ios Press.

Phoon, K.K. ed., 2008. Reliability-based design in geotechnical engineering: computations and applications. CRC Press.

Janbu, N., 1975, April. Slope stability computations: In Embankment-dam Engineering. Textbook. Eds. RC Hirschfeld and SJ Poulos. JOHN WILEY AND SONS INC., PUB., NY, 1973, 40P. In International Journal of Rock Mechanics and Mining Sciences & Geomechanics Abstracts (Vol. 12, No. 4, p. 67). Pergamon.

Bishop, A.W., 1955.The use of the slip circle in the stability analysis of slopes. Geotehnique 15(1),7–17.

Hungr, O., 1987. An extension of Bishop's simplified method of slope stability analysis to three dimensions. Geotechnique, 37(1), pp.113-117.

Fredlund, D.G., Krahn, J. and Pufahl, D.E., 1981, June. The relationship between limit equilibrium slope stability methods. In Proceedings of the International Conference on Soil Mechanics and Foundation Engineering (Vol. 3, pp. 409-416).

Kliche, C.A., 1999. Rock slope stability. SME.

Davis, R.O. and Selvadurai, A.P., 2005. Plasticity and geomechanics. Cambridge University Press.

Fenton, G.A. and Griffiths, D.V., 2008. Risk assessment in geotechnical engineering (Vol. 461). Hoboken, NJ: John Wiley & Sons.

Abderrahmane, T.H. and Abdelmadjid, B., 2016. Assessment of Slope Stability by Continuum and Discontinuum Methods. World Academy of Science, Engineering and Technology, International Journalof Civil, Environmental, Structural, Construction and Architectural Engineering, 10(4), pp.543-548.ssss

Depina, I., Le, T.M.H., Fenton, G. and Eiksund, G., 2016. Reliability analysis with metamodel line sampling. Structural Safety, 60, pp.1-15.

Lacasse, S., 2016. Hazard, Reliability and Risk Assessment-Research and Practice for Increased Safety. In Proceedings of the 17th Nordic Geotechnical Meeting Challenges in Nordic Geotechnic, Icelandic Geotechnical Society, Reykjavik (pp. 17-42).

Christian, J.T., Ladd, C.C. and Baecher, G.B., 1994. Reliability applied to slope stability analysis. Journal of Geotechnical Engineering, 120(12), pp.2180-2207.

Griffiths, D.V., Huang, J. and Fenton, G.A., 2010. Comparison of slope reliability methods of analysis. GeoFlorida 2010: Advances in Analysis, Modeling & Design (pp. 1952-1961).

Cederström, E.M.I.L., 2014. Application of probabilistic methods in slope stability calculations (Master's thesis, [E. Cederström]).

Christian, J.T. and Baecher, G.B., 1999. Point-estimate method as numerical quadrature. Journal of Geotechnical and Geoenvironmental Engineering, 125(9), pp.779-786.

Rosenblueth, E., 1975. Point estimates for probability moments. Proceedings of the National Academy of Sciences, 72(10), pp.3812-3814.

El-Ramly, H., Morgenstern, N.R. and Cruden, D.M., 2002. Probabilistic slope stability analysis for practice. Canadian Gesotechnical Journal, 39(3), pp.665-683.

Suchomel, R. and Mašın, D., 2010. Comparison of different probabilistic methods for predicting stability of a slope in spatially variable c–φ soil. Computers and Geotechnics, 37(1), pp.132-140.

Der Kiureghian, A., 2005. First-and second-order reliability methods. Engineering design reliability handbook, 14.

Wang, Y., Cao, Z. and Au, S.K., 2010. Practical reliability analysis of slope stability by advanced Monte Carlo simulations in a spreadsheet. Canadian Geotechnical Journal, 48(1), pp.162-172.

Davis, T.J. and Keller, C.P., 1997. Modelling uncertainty in natural resource analysis using fuzzy sets and Monte Carlo simulation: slope stability prediction. International Journal of Geographical Information Science, 11(5), pp.409-434.

Matsui, T. and San, K.C., 1992. Finite element slope stability analysis by shear strength reduction technique. Soils and foundations, 32(1), pp.59-70.

Griffiths, D.V. and Lane, P.A., 1999. Slope stability analysis by finite elements. *Geotechnique*, *49*(3), pp.387-403.

François, B., Bonnard, C., Laloui, L., Triguero, V., Zimmermann, T. and Truty, A., 2006. Numerical modeling of the hydro-mechanical behaviour of a large slope movement: the Triesenberg landslide (No. LMS-CHAPTER-2006-001). Elmepress Int.

Islam, M.R. and Faruque, M.O., 2012. Numerical modeling of slope stability consideration of an open-pit coalmine in the Phulbari coal basin, NW Bangladesh. Electronic Journal of Geotechnical Engineering (EJGE), 17, pp.3717-3729.

Sanavia, L., Sanavia, L., 2009. Numerical modelling of a slope stability test by means of porous media mechanics. Engineering Computations, 26(3), pp.245-266.

Fawaz, A., Farah, E. and Hagechehade, F., 2014. Slope stability analysis using numerical modelling. Am J Civ Eng, 2(3), pp.60-67.

MONI, M.M. and SAZZAD, M.M., 2015. Stability analysis of slopes with surcharge by LEM and FEM. International Journal of Advances in Structural and Geotechnical Engineering, 4(4), pp.216-225.

Pham, H.T. and Fredlund, D.G., 2003. The application of dynamic programming to slope stability analysis. Canadian Geotechnical Journal, 40(4), pp.830-847.

Griffiths, D.V., Huang, J. and Fenton, G.A., 2015. Probabilistic slope stability analysis using RFEM with non-stationary random fields. Risk V, Schweckendiek T, van Tol AF, Pereboom D et al (eds) Geotechnical Safety, pp.704-709.

Dawson, E.M., Roth, W.H. and Drescher, A., 1999. Slope stability analysis by strength reduction. Geotechnique, 49(6), pp.835-840.

Steinar Nordal, 2017. Geotechnical engineering advanced course. Geotechnical division of Norwegian University of Science and Technology (NTNU).

Calvello, M. and Cascini, L., 2006. Predicting rainfall-induced movements of slides in stiff clays.

Vardon, P.J., Liu, K. and Hicks, M.A., 2016. Reduction of slope stability uncertainty based on hydraulic measurement via inverse analysis. Georisk: Assessment and Management of Risk for Engineered Systems and Geohazards, 10(3), pp.223-240.

Sah, N.K., Sheorey, P.R. and Upadhyaya, L.N., 1994, February. Maximum likelihood estimation of slope stability. In *International journal of rock mechanics and mining sciences & geomechanics abstracts* (Vol. 31, No. 1, pp. 47-53). Pergamon.

Hsiao, E.C., Schuster, M., Juang, C.H. and Kung, G.T., 2008. Reliability analysis and updating of excavation-induced ground settlement for building serviceability assessment. Journal of Geotechnical and Geoenvironmental Engineering, 134(10), pp.1448-1458.

Vahdati, P., Levasseur, S., Mattsson, H. and Knutsson, S., 2013. Inverse soil parameter identification of an earth and rockfill dam by genetic algorithm optimization. In ICOLD European Club Symposium: 10/04/2013-12/04/2013.

Papon, A., Riou, Y., Dano, C. and Hicher, P.Y., 2012. Single-and multi-objective genetic algorithm optimization for identifying soil parameters. International Journal for Numerical and Analytical Methods in Geomechanics, 36(5), pp.597-618.

Dunnicliff, J., 1993. Geotechnical instrumentation for monitoring field performance. John Wiley & Sons.

Ho, A.N.L., Chan, E.K.K., Lau, K.W.K. and Sun, H.W., 2008, October. Instrumentation and real time monitoring of slope movement in Hong Kong. In Proceedings of the12th International Conference of International Association for Computer Methods and Advances in Geomechanics, Goa, India.

Stark, T.D. and Choi, H., 2008. Slope inclinometers for landslides. Landslides, 5(3), p.339.

DGSI. Durham Geo Slope Indicator, 2017. Inclinometers. [ONLINE] Available at: http://www.slopeindicator.com/instruments/inclin-intro.php. [Accessed 28 December 2017].

Millis, S.W., Ho, A.N.L., Chan, E.K.K., Lau, K.W.K. and Sun, H.W., 2008, October. Instrumentation and real time monitoring of slope movement in Hong Kong. In Proceedings of the12th International Conference of International Association for Computer Methods and Advances in Geomechanics, Goa, India.

Salewich, C., 2012. Real-time monitoring of a multiple retrogressive landslide (Doctoral dissertation).

Machan, G. and Bennett, V.G., 2008. Use of inclinometers for geotechnical instrumentation on transportation projects: State of the practice. Transportation Research E-Circular, (E-C129).

Wade, L.V. & Conroy, P.J. (1980). Rock mechanics study of a long wall panel. Mining Engineering, 12, 1728-1734.

Dowding, C.H. and O'Connor, K.M., 2000. Comparison of TDR and inclinometers for slope monitoring. In Geotechnical Measurements: Lab and Field (pp. 80-90).

Kane, W.F. and Beck, T.J., 2000. Instrumentation practice for slope monitoring. Engineering geology practice in Northern California. association of engineering geologists Sacramento and San Francisco sections, pp.1-20.

Damiano, E., Olivares, L. and Picarelli, L., 2012. Steep-slope monitoring in unsaturated pyroclastic soils. Engineering Geology, 137, pp.1-12.

Simoni, A., Berti, M., Generali, M., Elmi, C. and Ghirotti, M., 2004. Preliminary result from pore pressure monitoring on an unstable clay slope. Engineering Geology, 73(1), pp.117-128.

Huang, A.B., Lee, J.T., Ho, Y.T., Chiu, Y.F. and Cheng, S.Y., 2012. Stability monitoring of rainfall-induced deep landslides through pore pressure profile measurements. Soils and Foundations, 52(4), pp.737-747.

Vanneschi, C., Eyre, M., Francioni, M. and Coggan, J., 2017. The use of remote sensing techniques for monitoring and characterization of slope instability. Procedia engineering, 191, pp.150-157.

ISO, I., 2009. 31000: 2009 Risk management–Principles and guidelines. International Organization for Standardization, Geneva, Switzerland.

Baecher, G.B. and Christian, J.T., 2005. Reliability and statistics in geotechnical engineering. John Wiley & Sons.

Spross, J., Olsson, L., Hintze, S. and Stille, H., 2015. Hantering av geotekniska risker i byggprojekt: Ett praktiskt tillämpningsexempel.

Norwegian tunneling society, 2012. Contracts in Norwegian Tunneling, Publication 21.

Dai, F.C., Lee, C.F. and Ngai, Y.Y., 2002. Landslide risk assessment and management: an overview. Engineering geology, 64(1), pp.65-87.

Vardon, P.J., Liu, K. and Hicks, M.A., 2016. Reduction of slope stability uncertainty based on hydraulic measurement via inverse analysis. Georisk: Assessment and Management of Risk for Engineered Systems and Geohazards, 10(3), pp.223-240.

Calvello, M. and Finno, R.J., 2004. Selecting parameters to optimize in model calibration by inverse analysis. Computers and Geotechnics, 31(5), pp.410-424.

Honjo, Y., Wen-Tsung, L. and Guha, S., 1994. Inverse analysis of an embankment on soft clay by extended Bayesian method. International Journal for Numerical and Analytical Methods in Geomechanics, 18(10), pp.709-734.

Zentar, R.H.P.Y., Hicher, P.Y. and Moulin, G., 2001. Identification of soil parameters by inverse analysis. Computers and Geotechnics, 28(2), pp.129-144.

Bin, C., Ning, L. and Jia-shou, Z., 2004. Extended Bayesian method of inverse analysis in geoengineering. Chinese Journal of Rock Mechanics and Engineering, 23(4), pp.555-560.

Whitman, R.V., 2000. Organizing and evaluating uncertainty in geotechnical engineering. Journal of Geotechnical and Geoenvironmental Engineering, 126(7), pp.583-593.

Cao, M. and Qiao, P., 2008. Neural network committee-based sensitivity analysis strategy for geotechnical engineering problems. Neural Computing and Applications, 17(5-6), pp.509-519.

Stockholms Stad, 2017. [online] Slussen. Retrieved from: http://vaxer.stockholm.se/projekt/slussen/

Strålin, J., 2007. En bakgrund till skadorna på Slussens bärande konstruktioner.

ELU Konsult AB, 2017. [online] NYA SLUSSEN. Retrieved from: http://www.elu.se/reference/nya-slussen/

Karlsson, M. and Moritz, L., 2014. Trafikverkets tekniska krav för geokonstruktioner, TK Geo 13. Document, Trafikverket, Borlänge, SE.

Storstockholms Lokaltrafik AB, 2009. Säkerhetsbestämmelse, Lastförutsättningar för SL:s spårbärande byggnadsverk. SÄK-0288, Identitet SL-2009-11711.

8. Appendix

CPT test result:
16E001:

2017-01-27

C P T - sondering

Sida 1 av 1

Projekt			Plats	Östra väggen
Slussen			Borrhål	16E001 1(2)
50283			Datum	170102

Djup (m)				ρ	w_L	τ_{fu}	ϕ	σ_{vo}	σ'_{vo}	σ'_c	OCR	I_D	E	M_{OC}	M_{NC}
Från	Till	Klassificering		t/m³		kPa	°	kPa	kPa	kPa		%	MPa	MPa	MPa
0,00	2,40	FsaGr		1,80				21,2	21,2						
2,40	2,60	Cl M	NCSi	1,60		(42,1)		43,9	43,9		1,00				
2,60	2,80	Cl L	NCSi	1,60		(35,8)		47,1	47,1		1,00				
2,80	3,00	Cl H	NCSi	1,85		(83,5)		50,5	50,5		1,00				
3,00	3,20	Cl H	NC	1,85		(77,0)		54,1	54,1		1,00				
3,20	3,40	Si L		1,70		((99,7))	(31,5)	57,6	57,6				6,3	7,5	6,0
3,40	3,60	Si Med		1,80		((247,3))	(35,3)	61,0	61,0				14,3	18,2	14,6
3,60	3,80	Sa Med		1,90			37,7	64,6	64,6			66,4	29,3	39,3	31,5
3,80	4,00	Si Med		1,80		((186,6))	(33,7)	68,3	68,3				11,1	13,9	11,1
4,00	4,20	Si L		1,70		((142,5))	(32,5)	71,7	71,7				8,7	10,7	8,6
4,20	4,40	Cl H	NC	1,85		(79,8)		75,2	75,2		1,00				
4,40	4,60	Si L		1,70		((133,1))	(31,5)	78,7	77,2				8,2	10,0	8,0
4,60	4,80	Si L		1,70		((130,4))	(31,2)	82,0	78,5				8,1	9,9	7,9
4,80	5,00	Cl H	NC	1,85		(78,5)		85,5	80,0		1,00				
5,00	5,20	Cl H	NC	1,85		(86,8)		89,1	81,6		1,00				
5,20	5,40	Cl vL	NC	1,30		(17,7)		92,2	82,7		1,00				
5,40	5,60	Cl vL	NCSi	1,30		(18,4)		94,8	83,3		1,00				
5,60	5,80	Cl H	NC	1,90		(128,6)		97,9	84,4		1,00				
5,80	6,00	Si Med		1,80		((178,9))	(32,8)	101,5	86,0				10,8	13,5	10,8
6,00	6,20	Si Med		1,80		((206,5))	(33,7)	105,1	87,6				12,3	15,5	12,4
6,20	6,40	Si Med		1,80		((198,0))	(33,3)	108,6	89,1				11,9	14,9	11,9
6,40	6,60	Cl H	NCSi	1,90		(110,6)		112,2	90,7		1,00				
6,60	6,80	Cl vH	NCSi	1,90		(157,5)		116,0	92,5		1,00				
6,80	7,00	Si Med		1,80		((201,9))	(33,1)	119,6	94,1				12,1	15,2	12,2
7,00	7,20	Cl H	NCSi	1,90		(130,8)		123,2	95,7		1,00				
7,20	7,40	Sa Med		1,90			35,4	126,9	97,4			52,2	22,4	29,4	23,6
7,40	7,60	Cl vH	NCSi	1,90		(172,6)		130,7	99,2		1,00				
7,60	7,80	Sa Med		1,90			35,0	134,4	100,9			49,9	21,1	27,7	22,1
7,80	8,00	Sa Med		1,90			35,3	138,1	102,6			52,3	23,0	30,3	24,3
8,00	8,20	Sa L		1,80			32,8	141,8	104,3			34,3	12,9	16,3	13,0
8,20	8,40	Cl H	NC	1,90		(147,3)		145,4	105,9		1,00				
8,40	8,60	Si Med		1,80		((261,7))	(33,9)	149,0	107,5				15,4	19,7	15,8
8,60	8,80	Sa Med		1,90			34,6	152,6	109,1			48,2	20,7	27,1	21,7
8,80	9,00	Sa Med		1,90			34,8	156,4	110,9			50,3	22,3	29,4	23,5
9,00	9,20	Sa Med		1,90			35,5	160,1	112,6			55,1	26,3	35,1	28,0
9,20	9,40	Sa Med		1,90			36,1	163,8	114,3			60,1	31,1	42,0	33,6
9,40	9,60	Si Med		1,80		((254,1))	(33,2)	167,5	116,0				15,1	19,3	15,4
9,60	9,80	Si Med		1,80		((231,1))	(32,5)	171,0	117,5				13,9	17,6	14,1
9,80	10,00	Cl vH	NC	1,90		(171,2)		174,6	119,1		1,00				
10,00	10,20	Cl vH	NC	1,90		(169,2)		178,3	120,8		1,00				
10,20	10,40	Si Med		1,80		((312,0))	(33,5)	182,0	122,5				18,2	23,5	18,8
10,40	10,60	Cl vH	NC	1,90		(267,2)		185,6	124,1		1,00				
10,60	10,63	Si Med		1,80		((324,5))	(33,6)	187,7	125,1				18,8	24,5	19,6

2017-01-27

C P T - sondering

Sida 1 av 1

Projekt			Plats	Östra Väggen
Slussen			Borrhål	16E001 2(2)
50283			Datum	161230

Djup (m) Från	Till	Klassificering	ρ t/m³	w_L	τ_{fu} kPa	ϕ °	σ_{vo} kPa	σ'_{vo} kPa	σ'_c kPa	OCR	I_D %	E MPa	M_{OC} MPa	M_{NC} MPa
0,00	4,35	FsaGr	1,80				38,4	38,4						
4,35	14,60	FsaGr	1,80				167,3	116,1						
14,60	14,80	Si v L	1,60		((106,2))	(25,5)	259,4	155,9				7,4	9,0	7,2
14,80	15,00	Sa Med	1,90			34,4	262,8	157,3			52,3	28,1	37,6	30,1
15,00	15,20	Sa Med	1,90			35,0	266,5	159,0			56,7	32,5	44,0	35,2
15,20	15,40	Sa Med	1,90			35,7	270,3	160,8			61,4	38,1	52,2	40,9
15,40	15,60	Sa L	1,80			33,9	273,9	162,4			49,2	25,7	34,3	27,4
15,60	15,80	Sa D	2,00			38,0	277,6	164,1			83,0	77,4	111,8	64,7
15,80	15,84	Sa D	2,00			38,2	280,0	165,3			85,9	85,5	124,4	69,8

16E002:

C P T - sondering

Sida 1 av 1

Projekt			Plats	Östra väggen
Slussen			Borrhål	16E002 1(3)
50283			Datum	2017-01-17

Djup (m) Från	Till	Klassificering	ρ t/m³	w_L	τ_{fu} kPa	ϕ °	σ_{vo} kPa	σ'_{vo} kPa	σ'_c kPa	OCR	I_D %	E MPa	M_{OC} MPa	M_{NC} MPa
0,00	3,30	FgrSa	2,10				34,0	34,0						
3,30	6,00	FgrSa	2,10				95,8	82,3						
6,00	6,15	Sa Med	1,90			35,6	125,0	97,3			53,5	23,3	30,8	24,7

2017-01-27

C P T - sondering

Sida 1 av 1

Projekt			Plats	Östra väggen
Slussen			Borrhål	16E002 2(3)
50283			Datum	2017-01-18

Djup (m) Från	Till	Klassificering	ρ t/m³	w_L	τ_{fu} kPa	ϕ °	σ_{vo} kPa	σ'_{vo} kPa	σ'_c kPa	OCR	I_D %	E MPa	M_{OC} MPa	M_{NC} MPa
0,00	3,30	FsaGr	2,10				34,0	34,0						
3,30	10,20	FsaGr	2,10				139,1	104,6						
10,20	10,40	FsaGr	2,10				212,0	142,0						
10,40	10,60	Cl H NCSi	1,90		(147,9)		216,1	144,1		1,00				
10,60	10,80	Cl vH NC	1,90		(181,7)		219,8	145,8		1,00				
10,80	11,00	Cl vH NCSi	1,90		(184,7)		223,6	147,6		1,00				
11,00	11,20	Cl H NC	1,90		(91,0)		227,3	149,3		1,00				
11,20	11,40	Cl H NCSi	1,85		(77,4)		231,0	151,0		1,00				
11,40	11,60	Cl H NC	1,90		(115,2)		234,7	152,7		1,00				
11,60	11,80	Cl vH NC	1,90		(206,1)		238,4	154,4		1,00				
11,80	12,00	Cl H NC	1,90		(127,6)		242,1	156,1		1,00				
12,00	12,20	Cl H NCSi	1,90		(90,4)		245,8	157,8		1,00				
12,20	12,40	Cl vH NCSi	1,90		(258,5)		249,6	159,6		1,00				
12,40	12,44	Cl H NCSi	1,90		(128,9)		251,8	160,6		1,00				

2017-01-27

C P T - sondering

Sida 1 av 1

Projekt			Plats	Östra väggen
Slussen			Borrhål	16E002 3(3)
50283			Datum	2017-01-18

Djup (m) Från	Till	Klassificering		ρ t/m³	w_L	τ_{fu} kPa	ϕ °	σ_{vo} kPa	σ'_{vo} kPa	σ'_c kPa	OCR	I_D %	E MPa	M_{OC} MPa	M_{NC} MPa
0,00	3,30	FsaGr		2,10				34,0	34,0						
3,30	13,00	FsaGr		2,10				167,9	119,4						
13,00	13,20	Cl vH	NCSi	1,90		(266,3)		269,7	171,7		1,00				
13,20	13,40	Cl H	NCSi	1,90		(135,9)		273,4	173,4		1,00				
13,40	13,60	Cl vH	NCSi	1,90		(151,5)		277,1	175,1		1,00				
13,60	13,80	Cl H	NCSi	1,90		(119,2)		280,9	176,9		1,00				
13,80	14,00	Cl M	NCSi	1,85		(63,4)		284,5	178,5		1,00				
14,00	14,03	Si D		1,95		((441,5))	(33,4)	286,6	179,5				25,2	33,4	26,8

16E003:

2017-01-27

C P T - sondering

Sida 1 av 1

Projekt			Plats	Östra väggen
Slussen			Borrhål	16E003 1(2)
50283			Datum	161227

Djup (m) Från	Till	Klassificering		ρ t/m³	w_L	τ_{fu} kPa	ϕ °	σ_{vo} kPa	σ'_{vo} kPa	σ'_c kPa	OCR	I_D %	E MPa	M_{OC} MPa	M_{NC} MPa
0,00	4,50	FsaGr		1,80				39,7	39,7						
4,50	6,50	FsaGr		1,80				97,1	87,1						
6,50	6,70	Sa L		1,80			33,3	116,5	95,5			35,0	12,7	16,0	12,8
6,70	6,90	Cl vH	NCSi	1,90		(172,6)		120,2	97,2		1,00				
6,90	7,10	Sa Med		1,90			35,3	123,9	98,9			51,6	22,1	29,0	23,2
7,10	7,30	Sa Med		1,90			37,1	127,6	100,6			67,0	36,7	50,1	40,0
7,30	7,50	Sa Med		1,90			37,0	131,4	102,4			66,5	36,4	49,7	39,7
7,50	7,70	Si D		1,95		((362,7))	(34,8)	135,1	104,1				20,6	27,0	21,6
7,70	7,90	Cl vH	NCSi	1,90		(292,4)		138,9	105,9		1,00				
7,90	8,10	Sa Med		1,90			35,7	142,6	107,6			55,7	26,3	35,0	28,0
8,10	8,30	Sa Med		1,90			35,5	146,4	109,4			54,4	25,4	33,7	27,0
8,30	8,50	Sa Med		1,90			35,7	150,1	111,1			56,8	27,6	36,9	29,5

2017-01-27

C P T - sondering

Sida 1 av 1

Projekt			Plats	Östra Väggen
Slussen			Borrhål	16E003 2(2)
50283			Datum	161228

Djup (m) Från	Till	Klassificering		ρ t/m³	w_L	τ_{fu} kPa	ϕ °	σ_{vo} kPa	σ'_{vo} kPa	σ'_c kPa	OCR	I_D %	E MPa	M_{OC} MPa	M_{NC} MPa
0,10	4,50	FsaGr		1,80				38,8	38,8						
4,50	13,30	FsaGr		1,80				155,4	111,4						
13,30	13,50	Cl vH	NCSi	1,90		(159,6)		234,9	145,9		1,00				
13,50	13,70	Cl vH	NCSi	1,90		(194,2)		238,7	147,7		1,00				
13,70	13,90	Cl vH	NCSi	1,90		(201,8)		242,4	149,4		1,00				
13,90	14,10	Cl EH	NCSi	1,90		(388,5)		246,1	151,1		1,00				
14,10	14,30	Cl vH	NCSi	1,90		(181,4)		249,9	152,9		1,00				
14,30	14,50	Cl vH	NCSi	1,90		(222,6)		253,6	154,6		1,00				
14,50	14,66	Cl vH	NCSi	1,90		(298,2)		257,0	156,2		1,00				

Result from simplified point estimate method.

Point 1, $a = 0$, $b = 0$, $c = 0$

Elevation	$\Delta\delta_i$ for each month and elevation							
3.915	0.13	0.21	0.03	0.19	0.65	1.21	1.55	2.05
2.915	0.26	0.17	0.17	0.15	0.39	1.19	1.77	2.46
1.915	0.42	0.13	0.33	0.55	0.02	1.39	2.19	2.87
0.915	0.97	0.96	0.56	0.15	0.60	1.47	2.20	2.95
-0.085	1.21	0.79	0.89	0.83	1.29	1.69	2.18	2.91
-1.085	1.10	0.69	0.19	0.72	2.52	2.24	2.35	2.71
-2.085	2.12	1.05	0.19	0.58	0.54	1.25	1.25	0.15
-3.085	1.93	0.83	0.45	0.91	0.39	1.31	1.42	0.39
-4.085	0.83	0.00	1.21	1.97	1.24	2.33	2.35	1.68
-5.085	0.41	0.63	1.95	3.01	2.37	2.46	2.09	1.78
-6.085	0.10	0.60	1.63	2.52	2.01	1.45	1.23	1.06
-7.085	0.02	0.58	1.25	1.87	1.60	1.37	1.31	1.09
-8.085	0.13	0.63	1.68	2.70	2.26	2.18	1.98	1.69
-9.082	0.05	0.47	1.01	1.54	1.37	1.34	1.32	1.32
$\Delta\delta_{total}$	137.08 mm							
FS	2.204							

Point 2, $a = 1$, $b = 1$, $c = 1$

Elevation	$\Delta\delta_i$ for each month and elevation/mm							
3.915	0.10	0.16	0.08	0.32	0.75	1.29	1.61	2.11
2.915	0.29	0.07	0.05	0.17	0.69	1.46	2.03	2.72
1.915	0.44	0.19	0.07	0.09	0.48	1.83	2.61	3.29
0.915	0.95	0.95	0.71	0.61	1.09	1.95	2.67	3.42
-0.085	1.13	0.77	0.94	1.27	1.82	2.20	2.68	3.41
-1.085	0.99	0.65	0.28	1.10	2.94	2.64	2.75	3.10
-2.085	1.92	1.07	0.18	0.26	1.40	0.44	0.46	0.64
-3.085	1.77	0.93	0.07	0.04	1.29	0.47	0.60	0.42
-4.085	0.76	0.09	0.85	1.37	0.68	1.81	1.85	1.19

-5.085	0.37	0.52	1.58	2.40	1.81	1.95	1.61	1.31
-6.085	0.08	0.51	1.35	2.06	1.59	1.07	0.87	0.71
-7.085	0.02	0.53	1.08	1.58	1.33	1.14	1.08	0.87
-8.085	0.13	0.58	1.50	2.39	1.98	1.94	1.75	1.46
-9.082	0.06	0.47	0.98	1.48	1.31	1.29	1.28	1.28
$\Delta\delta_{total}$	131.8 mm							
FS	2.302							

Point 3, $a = -1$, $b = 1$, $c = 1$

Elevation	$\Delta\delta_i$ for each month and elevation/mm							
3.915	0.10	0.16	0.08	0.32	0.75	1.29	1.61	2.11
2.915	0.29	0.07	0.05	0.17	0.69	1.46	2.03	2.72
1.915	0.44	0.19	0.07	0.09	0.47	1.82	2.61	3.29
0.915	0.95	0.95	0.71	0.61	1.09	1.95	2.66	3.41
-0.085	1.13	0.77	0.94	1.27	1.81	2.20	2.68	3.41
-1.085	0.99	0.65	0.28	1.10	2.94	2.65	2.75	3.10
-2.085	1.92	1.07	0.18	0.26	1.41	0.43	0.46	0.64
-3.085	1.77	0.93	0.07	0.04	1.30	0.46	0.59	0.43
-4.085	0.76	0.09	0.85	1.36	0.67	1.81	1.85	1.18
-5.085	0.37	0.52	1.58	2.40	1.81	1.95	1.60	1.31
-6.085	0.08	0.51	1.35	2.06	1.59	1.07	0.87	0.71
-7.085	0.02	0.53	1.08	1.58	1.33	1.14	1.08	0.87
-8.085	0.13	0.58	1.50	2.39	1.98	1.93	1.74	1.46
-9.082	0.06	0.47	0.98	1.48	1.31	1.29	1.28	1.28
$\Delta\delta_{total}$	131.72 mm							
FS	2.295							

Point 4, $a = 1$, $b = -1$, $c = 1$

Elevation	$\Delta\delta_i$ for each month and elevation/mm							
3.915	0.24	0.34	0.20	0.00	0.52	1.12	1.48	1.99

2.915	0.13	0.38	0.48	0.53	0.06	0.89	1.49	2.19
1.915	0.27	0.09	0.69	1.06	0.45	0.95	1.77	2.46
0.915	0.78	0.69	0.17	0.47	0.00	0.88	1.61	2.36
-0.085	1.01	0.47	0.40	0.05	0.51	0.91	1.41	2.14
-1.085	0.99	0.44	0.28	0.10	1.60	1.33	1.44	1.80
-2.085	1.96	0.49	1.33	2.43	1.40	3.15	3.13	2.02
-3.085	1.84	0.27	1.72	2.90	1.60	3.22	3.29	2.24
-4.085	0.81	0.32	1.98	3.19	2.42	3.44	3.43	2.74
-5.085	0.40	0.92	2.69	4.20	3.49	3.50	3.09	2.76
-6.085	0.10	0.80	2.16	3.39	2.83	2.20	1.94	1.75
-7.085	0.01	0.70	1.57	2.41	2.10	1.83	1.74	1.51
-8.085	0.15	0.72	1.98	3.24	2.78	2.65	2.41	2.11
-9.082	0.05	0.48	1.05	1.62	1.46	1.41	1.40	1.39
$\Delta\delta_{total}$	165.96 mm							
FS	2.254							

Point 5, $a = 1$, $b = 1$, $c = -1$

Elevation	$\Delta\delta_i$ for each month and elevation/mm							
3.915	0.07	0.14	0.08	0.30	0.72	1.26	1.58	2.08
2.915	0.32	0.08	0.02	0.05	0.54	1.31	1.88	2.57
1.915	0.48	0.20	0.18	0.34	0.18	1.52	2.31	2.99
0.915	0.99	1.01	0.65	0.36	0.79	1.64	2.36	3.11
-0.085	1.18	0.83	1.00	1.12	1.53	1.90	2.38	3.11
-1.085	1.03	0.70	0.33	1.07	2.90	2.61	2.71	3.07
-2.085	1.98	1.14	0.25	0.27	1.40	0.44	0.46	0.64
-3.085	1.81	0.99	0.11	0.08	1.33	0.43	0.56	0.46
-4.085	0.78	0.11	0.83	1.33	0.64	1.77	1.81	1.15
-5.085	0.37	0.51	1.57	2.36	1.77	1.91	1.56	1.27
-6.085	0.08	0.51	1.34	2.02	1.56	1.04	0.84	0.68
-7.085	0.02	0.53	1.08	1.56	1.31	1.11	1.06	0.85
-8.085	0.13	0.57	1.49	2.35	1.94	1.89	1.70	1.42

-9.082	0.06	0.47	0.97	1.45	1.28	1.26	1.25	1.25
$\Delta\delta_{total}$	126.72 mm							
FS	2.216							

Point 6, $a = 1$, $b = -1$, $c = -1$

Elevation	$\Delta\delta_i$ for each month and elevation/mm							
3.915	0.19	0.31	0.20	0.08	0.42	1.02	1.37	1.88
2.915	0.19	0.34	0.53	0.74	0.19	0.64	1.24	1.94
1.915	0.36	0.03	0.81	1.45	0.90	0.49	1.30	1.99
0.915	0.91	0.87	0.15	0.88	0.49	0.38	1.10	1.86
-0.085	0.97	0.70	0.22	0.58	0.29	0.12	0.62	1.35
-1.085	1.14	0.60	0.11	0.28	1.40	1.14	1.26	1.62
-2.085	2.23	0.77	1.09	2.59	1.57	3.31	3.29	2.18
-3.085	2.04	0.46	1.58	2.94	1.66	3.29	3.35	2.30
-4.085	0.88	0.25	1.94	3.19	2.43	3.45	3.44	2.75
-5.085	0.44	0.88	2.68	4.18	3.48	3.50	3.09	2.76
-6.085	0.11	0.79	2.17	3.37	2.82	2.19	1.94	1.75
-7.085	0.02	0.70	1.58	2.39	2.09	1.82	1.73	1.50
-8.085	0.14	0.73	1.99	3.21	2.76	2.63	2.40	2.10
-9.082	0.05	0.47	1.05	1.61	1.45	1.40	1.38	1.38
$\Delta\delta_{total}$	163.34 mm							
FS	2.086							

Point 7, $a = -1$, $b = 1$, $c = -1$

Elevation	$\Delta\delta_i$ for each month and elevation/mm							
3.915	0.07	0.14	0.08	0.30	0.72	1.26	1.58	2.08
2.915	0.32	0.08	0.02	0.05	0.54	1.31	1.88	2.57
1.915	0.48	0.20	0.18	0.34	0.18	1.52	2.31	2.99

0.915	0.99	1.01	0.65	0.36	0.79	1.64	2.36	3.11
-0.085	1.18	0.83	1.00	1.12	1.53	1.90	2.38	3.11
-1.085	1.03	0.70	0.33	1.07	2.90	2.61	2.71	3.07
-2.085	1.98	1.14	0.25	0.27	1.40	0.44	0.46	0.64
-3.085	1.81	0.99	0.11	0.08	1.33	0.43	0.56	0.46
-4.085	0.78	0.11	0.83	1.33	0.64	1.77	1.81	1.15
-5.085	0.37	0.51	1.57	2.36	1.77	1.91	1.56	1.27
-6.085	0.08	0.51	1.34	2.02	1.56	1.04	0.84	0.68
-7.085	0.02	0.53	1.08	1.56	1.31	1.11	1.06	0.85
-8.085	0.13	0.57	1.49	2.35	1.94	1.89	1.70	1.42
-9.082	0.06	0.47	0.97	1.45	1.28	1.26	1.25	1.25
$\Delta\delta_{total}$	126.71 mm							
FS	2.216							

Point 8, $a = -1$, $b = -1$, $c = 1$

Elevation	$\Delta\delta_i$ for each month and elevation/mm							
3.915	0.22	0.33	0.19	0.02	0.54	1.14	1.50	2.01
2.915	0.16	0.36	0.45	0.50	0.09	0.92	1.52	2.23
1.915	0.29	0.06	0.67	1.07	0.47	0.93	1.75	2.44
0.915	0.80	0.71	0.19	0.45	0.03	0.90	1.63	2.39
-0.085	1.03	0.49	0.41	0.06	0.52	0.92	1.42	2.15
-1.085	0.99	0.44	0.28	0.11	1.59	1.32	1.44	1.79
-2.085	1.97	0.50	1.33	2.43	1.40	3.15	3.13	2.02
-3.085	1.85	0.27	1.71	2.90	1.60	3.22	3.28	2.23
-4.085	0.81	0.32	1.98	3.19	2.42	3.44	3.43	2.74
-5.085	0.40	0.92	2.69	4.20	3.49	3.50	3.09	2.76
-6.085	0.10	0.80	2.16	3.39	2.83	2.20	1.94	1.75
-7.085	0.01	0.70	1.57	2.41	2.10	1.83	1.73	1.50
-8.085	0.14	0.73	1.98	3.23	2.78	2.65	2.41	2.11
-9.082	0.05	0.48	1.05	1.62	1.46	1.41	1.40	1.39
$\Delta\delta_{total}$	166.17 mm							

FS	2.272

Point 9, $a = -1$, $b = -1$, $c = -1$

Elevation	$\Delta\delta_i$ for each month and elevation/mm							
3.915	0.19	0.31	0.20	0.08	0.42	1.02	1.37	1.88
2.915	0.19	0.34	0.53	0.74	0.19	0.64	1.24	1.94
1.915	0.36	0.03	0.81	1.45	0.90	0.49	1.30	1.99
0.915	0.91	0.87	0.15	0.88	0.49	0.38	1.10	1.86
-0.085	1.19	0.68	0.60	0.29	0.04	0.42	0.91	1.64
-1.085	1.14	0.60	0.11	0.28	1.41	1.14	1.26	1.62
-2.085	2.23	0.77	1.09	2.59	1.57	3.31	3.29	2.18
-3.085	2.04	0.46	1.58	2.94	1.66	3.29	3.35	2.29
-4.085	0.88	0.25	1.94	3.19	2.43	3.45	3.44	2.75
-5.085	0.44	0.88	2.68	4.18	3.48	3.50	3.09	2.76
-6.085	0.11	0.79	2.17	3.37	2.82	2.19	1.94	1.75
-7.085	0.02	0.70	1.58	2.39	2.09	1.82	1.73	1.50
-8.085	0.14	0.73	1.99	3.21	2.76	2.63	2.40	2.09
-9.082	0.05	0.47	1.05	1.61	1.45	1.40	1.38	1.37
$\Delta\delta_{total}$	164.21 mm							
FS	2.102							

TRITA TRITA-ABE-MBT-18477
ISSN 1100-7990
ISRN KTH/KRV/14/06-SE